学位論文

Studies on the function of outer arm docking complex ODA-DC in the regular arrangement of outer arm dynein

（鞭毛ダイニン外腕の周期的構築における
ドッキング複合体 ODA-DC の機能）

平成 25 年 12 月 博士（理学）申請

東京大学大学院理学系研究科
生物科学専攻

大和　幹人

Doctoral Dissertation

Studies on the function of outer arm docking complex ODA-DC in the regular arrangement of outer arm dynein

Doctoral Dissertation

Submitted to the Graduate School of Science, The University of Tokyo

Mikito Owa

December 2013

CONTENTS

Abbreviations

ATP: Adenosine triphosphate

BAC: Bacterial artificial chromosome

BMH: 1,6-Bismaleimidohexane

CBB: Coomassie brilliant blue

CCDC: Coiled coil domain containing

Cys: Cysteine

DRC: Dynein regulatory complex

DTT: Dithiothreitol

EGTA: *O,O'*-Bis(2-aminoethyl)ethyleneglycol-*N,N,N',N'*-tetraacetic acid

EM: Electron microscopy

GST: Glutathione S-transferase

HA: Hemagglutinin

HC: Heavy chain

HEPES: 2-[4-(2-Hydroxyethyl)-1-piperazinyl]ethanesulfonic acid

His: Histidine

HPLC: High pressure liquid chromatography

IAD: Inner arm dynein

IFT: Intraflagellar transport

IC: Intermediate chain

LC: Light chain

LC/MS/MS: Liquid chromatography - tandem mass spectrometry

MIA: Modifier of inner arms complex

MS: Mass spectrometry

OAD: Outer arm dynein

ODA-DC: Outer dynein arm docking complex

PCD: Primary ciliary dyskinesia

PIPES: Piperazine-1,4-bis(2-ethanesulfonic acid)

SDS: Sodium dodecyl sulfate

SDS-PAGE: SDS-polyacrylamide gel electrophoresis

TAP: Tris-acetate-phosphate

TCEP-HCl: Tris(2-carboxymethyl)phosphine hydrochloride

Tris: Tris(hydroxymethyl)aminomethane

Abstract

Motile cilia/flagella are hair-like organelles that are essential for various physiological activities. Ciliary/flagellar inner structure has a longitudinal periodicity of 96 nm, which is well conserved from protists to mammals. Ciliary/flagellar beating is driven by axonemal dyneins. Outer arm dynein (OAD) is arranged on the outer doublet microtubules every 24 nm. Periodic binding of OAD on specific loci is important for efficient ciliary/flagellar beating; however, the molecular mechanism that specifies OAD arrangement remains unclear. Previous studies using green alga Chlamydomonas reinhardtii have shown that the outer dynein arm docking complex (ODA-DC) is necessary for the OAD docking to the outer doublet. In this study, I found that the ODA-DC has an ellipsoidal shape ~24 nm in length. Binding assays of the ODA-DC to the axoneme and chemical crosslinking of the axoneme revealed that ODA-DC molecules cooperatively bind to the outer doublet in an end-to-end manner. When flagella of an ODA-DC-missing mutant supplied with ODA-DC upon gamete fusion, ODA-DC molecules bind to the axoneme from the proximal part to the distal part unidirectionally, followed by binding OAD. These results indicate that a cooperative association of the ODA-DC underlies the 24-nm periodicity of OAD.

General introduction

Eukaryotic cilia and flagella are multi-functional organelles that widely distribute in various organisms. They are classified into two types: motile and immotile ones. Motile cilia and flagella generate propulsive force for cell movements such as swimming of sperm, and generation of fluid flow in trachea, oviduct and cerebral ventricle. Immotile cilia play a role in chemo- and/or mechano-sensing at retinal photoreceptors, renal tubules, etc. These two types of cilia cooperatively function in some cases: during embryonic development, nodal cilia generate the leftward flow, which is sensed by perinodal sensory cilia as a determinant of the left-right axis (Nonaka et al., 1998, Yoshiba et al., 2012). Defects in assembly of ciliary/flagellar structure cause many human diseases such as male sterility, hydrocephaly, polycystic kidney disease, and *situs inversus* (these are termed primary ciliary dyskinesia [PCD]).

The inner structure of cilia and flagella, axoneme, is composed of nine doublet microtubules and two singlet microtubules (called “9+2” structure: Fig. 1; some types of cilia do not have a pair of singlet microtubule). Axonemal components (such as axonemal dyneins, radial spokes and dynein regulatory complex) are arranged on the outer doublet A tubule with an overall periodicity of 96 nm (Fig. 1). Among them, axonemal dyneins generate force for cilia/flagella

beating by sliding two adjacent outer doublets. Outer and inner arm dyneins are bound to the outer doublet A tubule, and they generate force against neighboring outer doublet B tubule with ATP hydrolysis.

Axonemal dyneins are best characterized in the green alga *Chlamydomonas reinhardtii*, in which at least seven inner arm dyneins (IAD, designated "a" to "g") and one outer arm dynein (OAD) have been identified. IAD and OAD have different structural and functional properties. IAD is composed of one or two heavy chains and several associated proteins (Kamiya, 2002). Each IAD is bound to its specific site on the A tubule every 96 nm (Bui et al., 2009). The phenotype of the mutants lacking IAD (*ida* mutants) indicates that IAD is important for generation of waves with large amplitude (Brokaw and Kamiya, 1987; Kamiya et al., 1991; Yagi et al., 2005). OAD comprises three heavy chains, two intermediate chains, and eleven distinct light chains as a large protein complex of ~2 MDa. Most of the subunits are conserved from protists to mammals (King, 2011). OAD binds to the A tubule every 24 nm. This 24-nm periodicity is completely conserved in essentially all organisms that possess OAD (Ishikawa et al., 2007; Nicastro et al., 2006). In mutants lacking OAD (*oda* mutants), flagellar beat frequency is reduced, suggesting that OAD is required for flagella to beat at high frequency (Brokaw, 1994).

Both IAD and OAD contribute to appropriate flagellar beating. However, the phenotype of *oda* mutants is more severe than that of *ida* mutants: *oda* mutants display the lowered swimming velocity at ~30% of wild type level, whereas *ida* mutants at 60-70%. This is because OAD is the most powerful axonemal dynein that generates ~2/3 of the total propulsive force of flagellar beating (Minoura and Kamiya, 1995). Most of PCD are caused by defect in OAD assembly, probably because of this OAD property (Afzelius, 2004; Fliegauf et al., 2007; Zariwala et al., 2008).

Two major questions remain to be answered regarding arrangements of axonemal dyneins. The first question is how axonemal dyneins are incorporated into the axoneme. A previous work revealed that IAD a, c, d and e are conveyed to flagella by intraflagellar transport (IFT, a cargo transport driven by kinesin II), but OAD is not (Piperno et al., 1996). However, some other studies have argued IFT-dependent transport of OAD (Qin et al., 2004; Hou et al., 2007; Ahmed et al., 2008). The second question is how the dyneins are bound to the specific sites on the outer doublet in a periodic manner. Regardless of dependence on IFT, dyneins need to be released into the flagellar matrix after entry to flagella. For the arrangement of dyneins in the flagellar cytoplasm onto the axoneme, some axonemal factors should be necessary to specify the binding sites. However, such

factors have not been identified yet.

In this study, to clarify how OAD is regularly arranged on the outer doublet, I focused on outer dynein arm docking complex (ODA-DC). The ODA-DC was identified as a protein complex that mediates OAD binding to the outer doublet (Takada and Kamiya, 1994; Takada and Kamiya, 1997). Electron microscopic observations showed that the ODA-DC forms a small projection at the OAD binding site in *Chlamydomonas* mutants lacking OAD (but retaining ODA-DC; e.g., *oda6*) (Kamiya, 1988; Takada and Kamiya, 1994; Takada and Kamiya, 1997). In addition, the ODA-DC was suggested to be linearly arrayed every 24 nm along the outer doublet (Wakabayashi et al., 2001; Ishikawa et al., 2007).

I thus postulated that the ODA-DC contributes to not only the binding of OAD to the outer doublet, but also the periodic arrangement on the specific site. In this study, I analyzed the properties of the ODA-DC to test this hypothesis. In Part I, I characterized the biochemical properties of the ODA-DC molecules using the recombinant protein complex. I revealed that the ODA-DC has an ellipsoidal shape ~24 nm in length, and weakly associates with each other. Next, in Part II, I investigated binding manners between the ODA-DC and microtubules/axonemes. I found that the ODA-DC binds to the outer doublet from the proximal portion to the

distal portion in a positively cooperative manner. From these results, I propose a new model that the ODA-DC functions as a determinant of 24 nm periodicity of OAD.

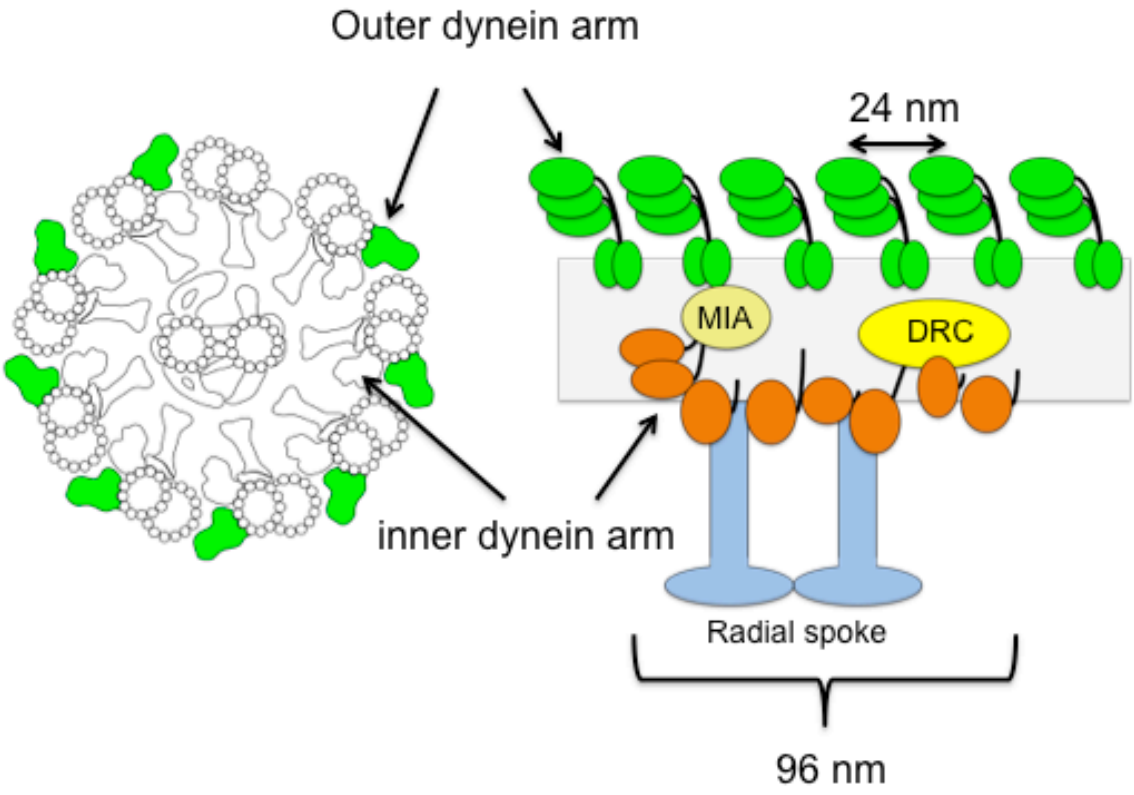

Figure 1

Schematic diagram of the axoneme. Left: cross sectional view of the axoneme. Right: longitudinal view of the outer doublet microtubule. Axonemal components such as OAD, IAD, radial spoke, DRC etc. aligned periodically within a 96 nm-unit of the outer doublet.

Part I

The molecular characteristics of the ODA-DC

Summary

The ODA-DC is the protein complex essential for OAD docking to the microtubule and the outer doublet. Previous studies using *Chlamydomonas* reported that the ODA-DC is composed of three subunits, DC1, DC2 and DC3, in a stoichiometry of 1:1:1. However, the biochemical properties of the ODA-DC remain poorly understood. In this section, I described the characteristics of the ODA-DC. An ultracentrifugation analysis and rotary shadowing of recombinant ODA-DC revealed that ODA-DC is a heterotrimer, and has an ellipsoidal shape ~24 nm in length. These results raise the possibility that the size of the ODA-DC itself determines 24 nm-periodicity of OAD.

Introduction

The binding between OAD and doublet microtubules is mediated by the ODA-DC. Takada and Kamiya first identified the ODA-DC as a projection at the OAD docking site (Takada and Kamiya, 1994). They demonstrated that a fraction from the sucrose density gradient centrifugation of the wild type extract containing the ODA-DC is necessary for OAD reconstitution on the *oda1* axoneme, which lacks both the ODA-DC and OAD.

In *Chlamydomonas*, the ODA-DC is composed of three subunits: DC1, ~83 kDa, encoded by *ODA3*; DC2, ~62 kDa, encoded by *ODA1*; and DC3, ~21 kDa, encoded by *ODA14* (Casey et al., 2003b; Koutoulis et al., 1997; Takada et al., 2002). DC1 and DC2 are coiled coil proteins, which are essential for the OAD docking on the microtubule because the mutants lacking these proteins (*oda1*, *oda3*) perfectly lack OAD on the mutant axonemes. In contrast, DC3, a redox-sensitive Ca^{2+} binding protein, is not necessary for OAD docking because the mutant (*oda14*, totally lacking DC3) retains OAD ~40% of wild-type level (Casey et al., 2003a; Casey et al., 2003b). Since the amounts of DC1 and DC2 are slightly reduced in the *oda14* mutant axoneme (~80% of their level in the wiled type axoneme, Casey et al., 2003b), DC3 presumably functions in stabilization of the ODA-DC. Among the subunits, DC2 is well conserved throughout evolution,

and seems to have undergone duplication in humans (CCDC63 and CCDC114) (Pazour et al., 2006). Recently, CCDC114 was shown to be one of the responsible genes of PCD and expressed in cilium-producing cells, whereas CCDC63 is almost expressed in testis (Onoufriadis et al., 2013). In the patients with defects in CCDC114, cilia of respiratory epithelial cells completely lack OAD (Knowles et al., 2013; Onoufriadis et al., 2013), suggesting that DC2 also functions in OAD docking to the axoneme in humans.

Thus, ODA-DC is generally required for OAD docking to the outer doublet. However, details of the ODA-DC properties are still poorly understood. Here, I analyzed the structural properties of the ODA-DC by using the recombinant ODA-DC (herein after referred to as DC1-2-3). I found that the ODA-DC is a heterotrimer with an ellipsoidal shape ~24 nm in length. Since the length is consistent with the periodicity of OAD, 24 nm, the interval of OAD on the axoneme could be determined the size of the ODA-DC.

Materials and Methods

Strains and culture of Chlamydomonas reinhardtii *cells*

A *Chlamydomonas reinhardtii* mutant *oda2* (lacking outer arm dyneins with a mutation in the structural gene of γ-HC) was used in this part. Cells were grown in Tris-acetate-phosphate (TAP) medium (Gorman and Levine, 1965) with aeration at 25°C, on a 12h/12h light/dark cycle (Gorman and Levine, 1965).

Preparation of Chlamydomonas *axonemes*

Chlamydomonas cells were vortexed (at 1400 rpm using EYELA MS-1000, Tokyo RikaKikai co., LTD) in HMS (10 mM HEPES pH 7.4, 5 mM $MgSO_4$, 4% sucrose) containing 8 mM dibucaine-HCl for 10 sec, followed by adding EGTA (2 mM final). After removal of cell bodies by centrifugation at 1,080 ×g for 6 min at 4°C, flagella were harvested by centrifugation at 27,000 ×g for 14 min at 4°C. Isolated flagella were demembranated with HMEK (30 mM HEPES pH 7.4, 5 mM $MgSO_4$, 1 mM EGTA, 50 mM K-acetate) containing 0.2% IGEPAL® CA-630 (Sigma Aldrich, 18896) and protease inhibitors for 10 min. after removal of the membrane and matrix fraction, axonemes were suspended with HMEK containing protease inhibitors.

Generation and purification of recombinant DC1-2-3

Bacterially expressed GST-DC3 (Casey et al., 2003b) was purified with Glutathione Sepharose 4B (GE Healthcare, 17-0756-01) and treated with PreScission Protease (GE Healthcare, 27-0843-01) to cleave off GST. A mixture of GST, DC3 and protease was mixed with insect culture cell lysate containing DC1 and DC2-6×His produced by the Baculovirus system (Ide et al., 2013), followed by purification on a Ni-NTA agarose column. (For DC1-2 purification, GST-DC3 was not added.)

Protein electroporation

Purified DC1-2-3 was dialyzed against HMDCaKS (30mM HEPES, 5mM MgSO4, 1mM DTT, 50mM K-acetate, 1mM Ca-acetate, 60mM sucrose, pH 7.4) and introduced into *oda3ida4* cells by modified method of Hayashi et al., 2002. Electroporation was carried out at 350 V-25 ohms-600 μF, using ECM630 (BTX, San Diego, CA). After pulse application, cuvettes were incubated at 15°C for 30 min with stirring every 5 min. The cells were then suspended in 500 μl TAP medium with 60 mM sucrose and left at room temperature. 2.5 hours after pulse application, the swimming cell number was counted.

Gel filtration chromatography

Gel filtration chromatography was used to compare the fluid dynamic properties of the native ODA-DC and DC1-2-3. The protein samples were applied to a Superose 6 HR gel–filtration column (Pharmacia Biotech, Uppsala, Sweden) using a Biologic Chromatography System HPLC apparatus (Bio-Rad, Hercules, CA) at a flow rate of 0.2 ml/minute.

Electron microscopy

Isolated axonemes and axonemes mixed with DC1-2-3 were fixed with 2% glutaraldehyde and 1% tannic acids. The Samples were post-fixed with 1% OsO_4, dehydrated with a series of ethanol solutions, and embedded in Epon 812. Sections were stained with uranyl acetate and lead citrate. DC1-2-3 molecules were imaged by low angle rotary shadowing electron microscopy using the method of Matsui et al. (Matsui et al., 2006). Purified DC1-2-3 in HMDEK was mixed with equal volume of glycerol, and samples were sprayed, using an airbrush, onto cleaved mica. The droplets on the mica were dried at room temperature in a vacuum at 10^{-8} mmHg in freeze-etch equipment (Hitachi HR7000) for 10 min. Dried specimens were rotary-shadowed with platinum using an electron gun positioned at 2.5° to the mica surface, and then coated with a film of carbon generated by an electron gun positioned at 90° to the mica surface. The replica was

floated on distilled water and collected on a grid covered with Formvar film. All samples were observed and photographed by an electron microscope JEM-1011 (JEOL, Tokyo, Japan). The length of DC1-2-3 was measured using Image J.

Analytical ultracentrifugation

Sedimentation velocity experiments were performed in an Optima XL-I analytical ultracentrifuge (Beckman-Coulter, CA, USA; 50Ti rotor, 40,000 rpm, 20°C). Moving boundaries were recorded at a wavelength of 390 nm without time intervals between successive scans. Sedimentation coefficient distribution function c(s) were calculated by SEDFIT program (Schuck, 2000). The molecular mass distribution c(M) was obtained by converting c(s) on the assumption that the frictional ratio f/f0 was common to all the molecular species as implemented in SEDFIT. The protein partial specific volume was calculated from the amino acid sequence; the buffer density and viscosity were calculated according to the solvent composition using the program SEDNTERP (Laue et al., 1992).

Results

Properties of DC1-2-3

DC1-2-3 was prepared by combining bacterially expressed DC3 (Casey et al., 2003b) with the DC1-DC2-6×His complex (referred to as "DC1-2") co-expressed in *sf21* insect culture cells (Ide et al., 2013), followed by purification on a Ni-NTA agarose column. The eluates contained DC1, DC2-6×His, and DC3, verifying that DC1-2-3 is purified as a single complex (Fig. I-1a).

By several criteria, I ascertained that the structural and functional properties of DC1-2-3 are identical to those of the native ODA-DC. First, the stoichiometry of the three subunits in DC1-2-3 estimated from the band intensities in SDS-polyacrylamide gel (assuming that all subunits have the same affinity for Coomassie brilliant blue) was 1:1:1, which is the same as that of the native ODA-DC (Takada et al., 2002). Second, the elution profile of DC1-2-3 from a gel filtration column is similar to that of the native ODA-DC, suggesting the structural similarity of the recombinant and native complex (Fig. I-1b). Third, DC1-2-3 rescued the phenotype of the *oda3ida4* (lacking ODA-DC, outer arm dyneins, inner arm dyneins a, c, and d; non-motile) when introduced by electroporation-mediated protein delivery. A few hours after introduction of DC1-2-3, ~19% of cells became motile (n=2735) whereas all control cells (pulse

application without proteins) remained non-motile (n=862). Finally, when DC1-2-3 was added to isolated axonemes of the *oda1* mutant, the projections identical to the ODA-DC in *oda6* axonemes were observed by thin-section electron microscopy (Fig. I-2c-e, arrows), suggesting preferentially reconstitution of the DC1-2-3 on the doublet microtubules (Fig. I-2a, arrows) (Takada and Kamiya, 1994).

The ODA-DC is a heterotrimer

As described above, I demonstrated that the stoichiometry of ODA-DC is 1:1:1, but the number of each subunit contained in a complex is not revealed. Then, I carried out analytical ultracentrifugation of DC1-2-3. Calculation of the molecular mass from the sedimentation velocity resulted in an estimate of ~152 kDa (Fig. I-3). This value is close to the sum of predicted molecular masses of DC1, DC2 and DC3 (~167 kDa), further suggesting that DC1-2-3 is a heterotrimer.

The ODA-DC has an ellipsoidal shape with ~24 nm in length

To obtain the information about the shape of DC1-2-3, I performed low-angle rotary shadowing electron microscopy. The observation after fixation with 0.1% glutaraldehyde revealed that DC1-2-3 has an ellipsoidal shape (Fig. I-4a,

b). The major axis length of these particles was normally distributed with a mean of ~28 nm (Fig. I-4c). Considering the thickness of the platinum coating, 2 nm on all sides, the actual mean length of DC1-2-3 is estimated to be ~24 nm.

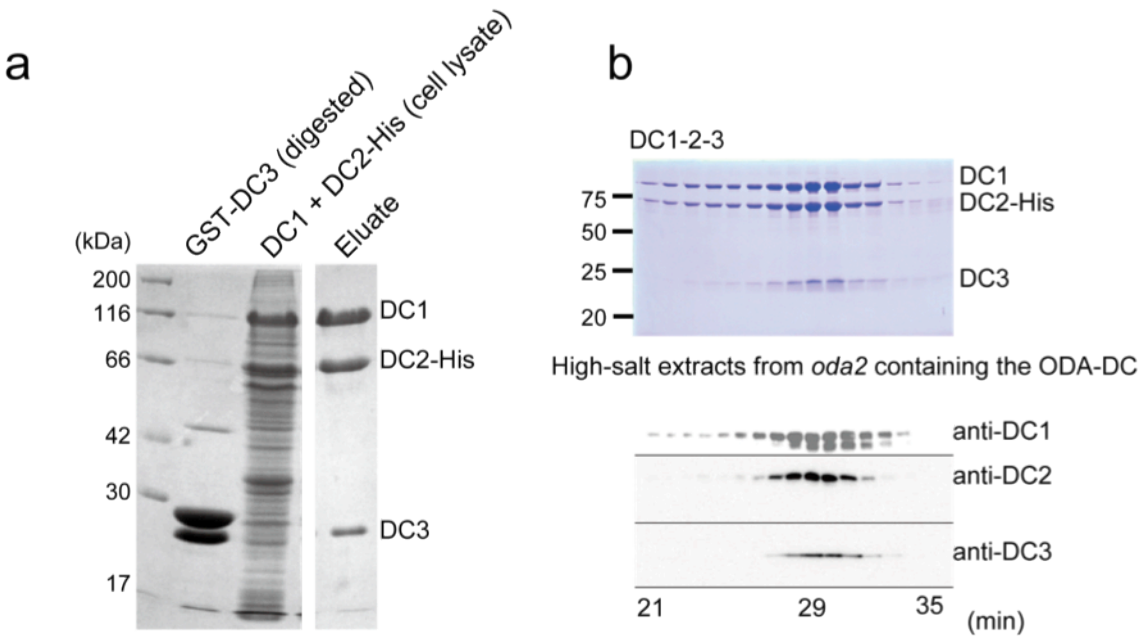

Figure I-1

(a) SDS-PAGE of recombinant ODA-DC (DC1-2-3) stained with Coomassie blue. DC1 and DC2-6×His co-expressed in *Sf21* insect cells were mixed with bacterially expressed GST-DC3 after digestion with protease to cleave off GST, and then purified using a Ni-NTA column. The resultant DC1+DC2-6×His+DC3 complex (termed DC1-2-3) contains equimolar amounts of the three proteins (DC1 : DC2 : DC3=1.0 : 0.89 : 0.92). (b) Gel-filtration column chromatography fractions of DC1-2-3 (top, Coomassie blue-stained gel) and the native ODA-DC extracted from *oda2* axonemes (bottom, Western blot probed with antibodies for each subunit). For each sample, fractions from 21 to 35 min were subjected to SDS-PAGE or Western analysis. The elution patterns of DC1-2-3 and native ODA-DC were almost the same, indicating the structural similarity of the two complexes.

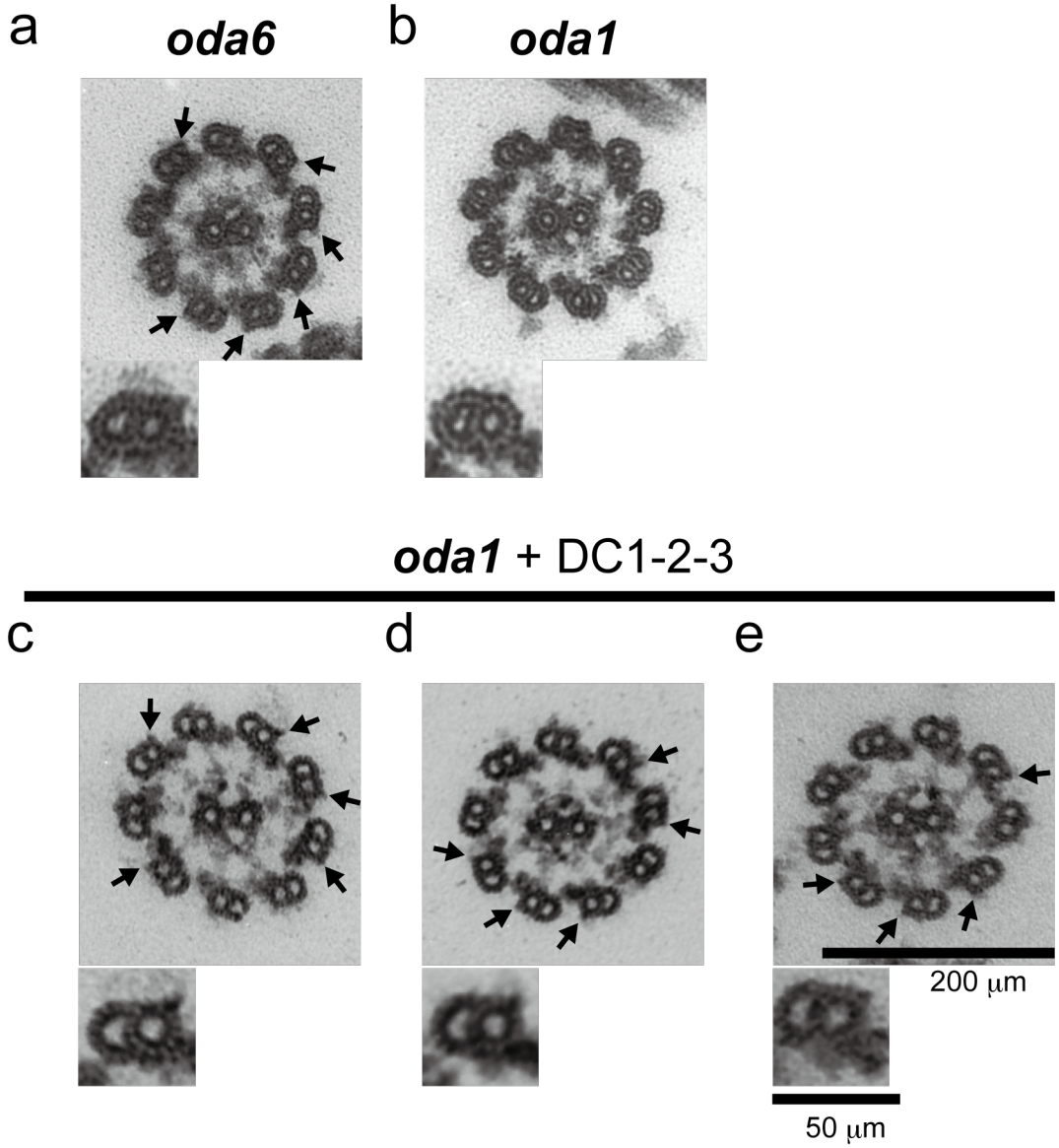

Figure I-2

Thin-section EM images of axonemes: (a) *oda6*, lacking OAD but having the ODA-DC; (b) *oda1*, lacking both OAD and the ODA-DC; and (c-e) *oda1* mixed with DC1-2-3. The bottom small panels show representative doublets. The projections (arrows) were observed at the same site on the doublets as the native ODA-DC on the *oda6* axoneme (a, arrows).

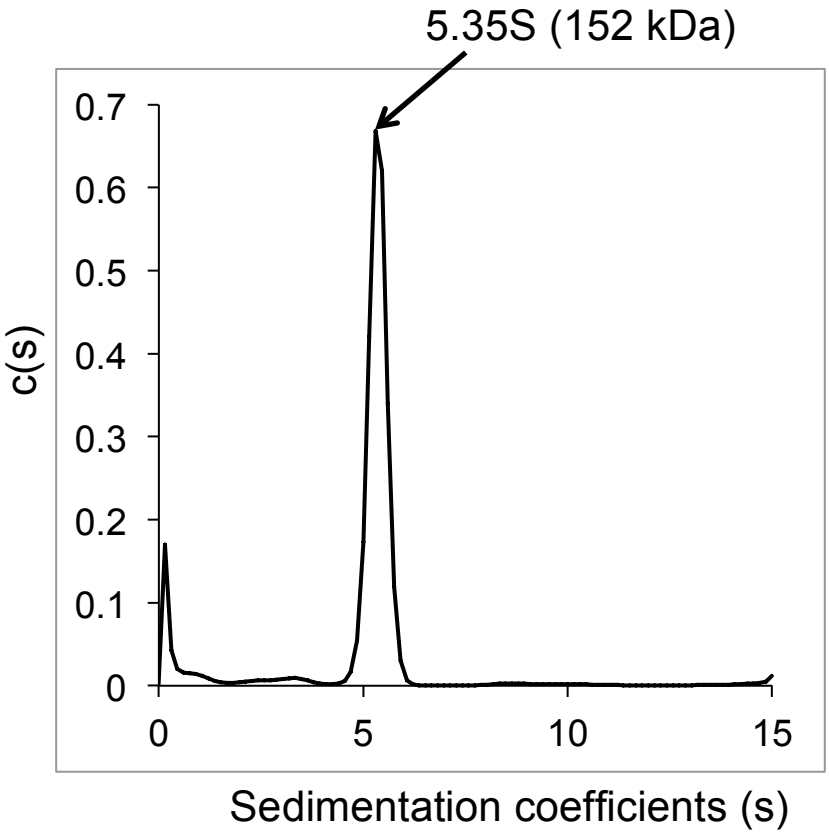

Figure I-3

Sedimentation coefficient distribution function c(s) was obtained from sedimentation velocity data by SEDFIT. c(s) was converted to c(M) to estimate the molecular mass of DC1-2-3 to be ~152 kDa.

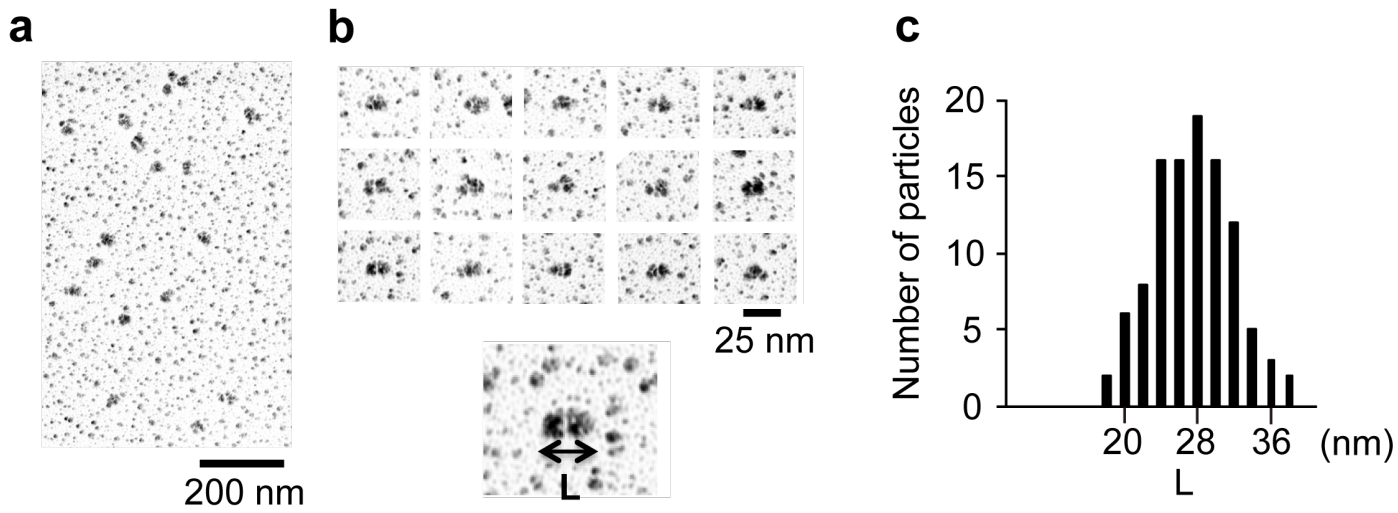

Figure I-4

(a) Low-magnification EM images of DC1-2-3 prepared by low angle rotary shadowing. (b) Typical images of DC1-2-3. Each particle has an ellipsoidal shape. (c) Histogram of the major axis length of DC1-2-3 (L) (n=108). Considering the thickness of platinum coating (2 nm on all sides), the peak length is ~24 nm.

Discussion

In this part, I examined the biochemical and structural properties of ODA-DC molecule using recombinant ODA-DC (DC1-2-3). Rotary shadowing observations showed that DC1-2-3, which is a heterotrimer identical to the native ODA-DC, has an ellipsoidal shape. The lengths of the long axis of DC1-2-3 molecule were normally distributed, with the peak at ~24 nm (after subtraction of 4 nm for thickness of platinum coating), which is parallel to the interval of OAD on the axoneme (Fig. I-4c). (Particles of <24 nm might represent DC1-2-3s broken during sample preparation, and those of >24 nm might have been fixed less well with glutaraldehyde and have a perturbed [or extended] structure presumably caused by mica surface charge [Goodenough and Heuser, 1984].) These data raise a possibility that ODA-DC is the determinant of the 24-nm periodicity.

DC1-2-3 introduction into the *oda3ida4* cells rescued its phenotype, demonstrating that DC1-2-3 retains the functions as the ODA-DC. In addition, the motility recovery was higher level (~19%) than when DC1-2 was introduced (<2%, Ide et al., 2013). These results suggest that DC3 stabilizes DC1-2-3 complex. Actually, in the axonemes of *oda14* (mutated in the DC3 gene and totally lacking DC3), the amounts of DC1 and DC2 are reduced by ~20% of their levels in the

wild type axonemes (Casey et al., 2003b). Furthermore, in *oda14* axonemes the outer arm dynein is also reduced by less than half of the normal level (Casey et al., 2003b), indicating that stability of the ODA-DC is required for proper building of the outer arm.

It is important to note that DC1-2-3 was preferentially reconstituted onto the specific site of *oda1* axoneme (Fig. I-2). This is consistent with the result showed in a previous study, that ODA-DC binding is limited to the specific site (Takada and Kamiya, 1994). These data suggest that some axonemal factor(s) may specify the binding site of the ODA-DC.

Part II

Cooperative binding of the ODA-DC to the microtubule

Summary

OAD is bound to the outer doublet microtubules every 24 nm. Periodic binding of OAD at specific sites should be essential for efficient cilia/flagella beating; however, the basis for the regular arrangement remains to be elucidated. By chemical crosslinking of mutant axonemes that lack OAD but retain the ODA-DC, I found that ODA-DCs are aligned in an end-to-end manner along the doublets. In vitro binding assays of DC1-2-3 to *oda1* axonemes (totally lacking the ODA-DC) and cytoplasmic microtubules revealed that the ODA-DC binds to them in a positively cooperative manner. When *oda1* is supplied with ODA-DC upon gamete fusion, binding of ODA-DCs to the mutant axonemes gradually proceeds from the proximal region to the tip, followed by binding of OAD. These results indicate that a cooperative association of the ODA-DC underlies its function as the OAD docking site and is the determinant of the 24-nm periodicity.

Introduction

The ODA-DC is essential for OAD docking to the outer doublet, although OAD itself binds directly to the microtubule via the C terminus region of intermediate chain 1 (IC1) (King et al., 1991; Ide et al., 2013). In high-salt extracts from wild type axonemes under the condition containing Mg^{2+}, OAD combines with the ODA-DC in a 1:1 stoichiometry (Takada et al., 2002). The ODA-DC captures OAD via at least three interactions between subunits of each complex (DiBella et al., 2004; Ide et al., 2013). However, the ODA-DC is assembled in cytoplasm independently of OAD and transported into the flagella independently of OAD (Wakabayashi et al., 2001). In addition, in the flagella of *oda* mutants retaining the ODA-DC but not OAD, the ODA-DC is arranged every 24 nm along the outer doublet (Wakabayashi et al., 2001; Ishikawa et al., 2007). Considering that OAD requires the ODA-DC for the docking to the doublet, these data raise a possibility that the arrangement of ODA-DC on the doublet is prior to that of OAD. Furthermore, as described in Part I, the length of the ODA-DC is ~24 nm, the same value as OAD interval. From these results, I postulate that 24-nm periodicity of OAD is produced by the regular arrangement of the ODA-DC.

To test this hypothesis, I investigated the microtubule-binding properties

of the ODA-DC by using recombinant proteins as well as native proteins, and also observed how ODA-DC and OAD are incorporated into axonemes in vivo. I found that ODA-DCs associate with each other on the doublet microtubules and that the binding of the ODA-DC proceeds from the base of the axoneme to the tip. I propose that these properties are the basis for the ordered arrangement of OAD.

Material and Methods

Strains

A *Chlamydomonas reinhardtii* wild-type strain (CC124) and the following mutants lacking outer dynein arms (Kamiya, 1988) were used: *oda1*, with a mutation in the structural gene of DC2, lacking the ODA-DC (Takada et al., 2002); *oda2*, with a mutation in the structural gene of the g-HC, lacking outer arm dynein; *oda6*, with a mutation in the structural gene of the ODA intermediate chain IC2, lacking outer arm dynein (Mitchell and Kang, 1991). Double mutants were produced by standard procedures (Harris, 1989). All cells are grown as described by Part I.

Generation of oda1oda6::ODA1-3×HA strain

The *ODA1* gene was amplified from a BAC library (#PTQ12942) of the *Chlamydomonas* genome, and an NruI site was inserted immediately in front of the stop codon. A 3×HA tag fragment was inserted at the NruI site and, together with the plasmid pSI103, used to co-transform the non-motile double mutant *ida2oda1* (Sizova et al., 2001). Rescued strains that displayed the slow-swimming phenotype of *ida2* were isolated and mated with *oda1oda6*. *oda1oda6*::ODA1-3×HA was selected from the progeny as a clone that had an HA epitope and displayed jerky

swimming typical of an *oda* mutant.

Preparation of porcine brain tubulin and cytoplasmic microtubules

Tubulin was purified from porcine brain by cycles of assembly and disassembly in vitro in a high-molarity PIPES buffer using the method of Castoldi and Popov (Castoldi and Popov, 2003). Microtubule pellets were resuspended in HMEKCl (30 mM HEPES, 5 mM $MgSO_4$, 1 mM EGTA, 0.1 M KCl, pH 7.4) containing 10 μM paclitaxel.

Co-sedimentation of recombinant proteins with axonemes and microtubules

The binding of the recombinant proteins to axonemes and microtubules was assessed by centrifugation followed by SDS-PAGE and Western blotting. DC1-2-3 samples purified with Ni-NTA resin (cOmplete His-tag Purification Resin, Roche) and a Uno Q1 column (Bio-Rad) were dialyzed against HMEKCl and mixed with axonemes or porcine brain cytoplasmic microtubules. After incubation at 4℃ (axonemes) or 25℃ (microtubules) for 60 min in HMEKCl containing 0.1% Tween 20, the mixture was centrifuged at 19,000 × g for 15 min at 4℃ for axonemes or 100,000 × g for 20 min at 25℃ for microtubules. The precipitates were resuspended in HMEKCl, mixed with an equal volume of 2× SDS-sample buffer, boiled for 3 min, and analyzed by SDS-PAGE and Western blotting with anti-His-tag antibody (MBL D291-3). The amount of bound DC1-2-3

was calculated from the band intensity of DC2-His in Western blots using a calibration curve generated from purified DC1-2-3 of known concentrations. The estimated molar ratio of the DC1-2-3 bound to the *oda1* axonemes compared to the ODA-DC contained in the same amount of wild-type axonemes was multiplied by 8/9 (this is because one of the nine outer doublets has no ODA-DC and OAD in the wild-type axoneme. For calculation of the amount of the ODA-DC contained in the wild-type axoneme, the ODA-DC and purified DC1-2-3 used for calibration were immuno-detected with anti-DC2 antibody and their intensities were compared. The amount of DC1-2-3 bound to the cytoplasmic microtubule per 24 nm was estimated from the molar ratio of the bound DC1-2-3 to total tubulin monomers (α + β tubulins); the molar ratio was multiplied by 78 because a cytoplasmic microtubule contains 78 tubulin molecules per 24 nm (6 tubulin monomers × 13 protofilaments).

Labeling and fluorescence microscopy

Purified DC1-2-3 was mixed with 10-fold molar excess of Alexa-488 maleimide (Sigma-Aldrich, A10254) for 1 hour at room temperature. The reaction was quenched by addition of 5 mM TCEP-HCl (*tris*(2-carboxyethyl)phosphine hydrochloride), and then free Alexa-488 maleimide was removed by Ni-NTA

purification. Immunofluorescence microscopy was carried out as previously described (Sanders and Salisbury, 1995). Temporary dikaryons were allowed to adhere to a slide glass, demembranated with Igepal-CA630 (Sigma, 18896), and fixed with 2% w/v paraformaldehyde. The antibodies used were anti-HA tag antibody (1:100, Roche Applied Science, 1583816), and anti-IC2 antibody (1:100, Sigma-Aldrich, D6168). The secondary antibodies used were anti-mouse IgG antibody conjugated with Alexa Fluor 594 (1:500, Invitrogen, A11005) and anti-mouse IgG antibody conjugated with Alexa Fluor 350 (1:200, Invitrogen A11045). All fluorescence images were collected using an upright fluorescence microscope (Axioplan, Zeiss) equipped with a Plan-Apochromat (×63, 1.40 NA) objective and a CCD camera (COOL SNAP, Photometrics). The camera was controlled by Micro-Manager 1.4. Fluorescence intensity of microtubules was measured by Image J.

Chemical crosslinking, immunoprecipitation and SDS-PAGE

Chemical crosslinking and immunoprecipitation were used to detect molecular interaction between different ODA-DC subunits. The axonemes of *oda6*, the mixture of DC1-2-3 and cytoplasmic microtubules, or DC1-2 were treated with 1, 6-Bismaleimidohexane (BMH, Thermo Scientific) for 60 min at room

temperature. After the reaction was quenched with excess 2-mercaptoethanol, the samples were centrifuged at 19,000 × g for 15 min at 4℃. OAD and the ODA-DC were released from the axoneme by suspending the pellets in high salt HMEKCl (30 mM HEPES, 5 mM $MgSO_4$, 1 mM EGTA, 0.6 M KCl, pH 7.4). The suspension was incubated for 10 min at 4℃, centrifuged at 19,000 × g for 10 min at 4℃, and the supernatant mixed with the sample buffer, boiled, and analyzed by SDS-PAGE (the length of separating gel was 9.5 cm for axonemal samples, or 5.5 cm for DC1-2 and cytoplasmic microtubule samples) and Western blotting. The antibodies used were anti-DC1 antibody, anti-DC2 antibody, anti-DC3 antibody, anti-a-tubulin antibody (Sigma, T6074), and anti-b-tubulin antibody (Sigma, T0198). The crosslinked samples were immunoprecipitated with anti-DC1 antibody following a previously described method (King et al., 1991; Wakabayashi et al., 2001). The apparent molecular masses of the detected bands were calculated by Image J.

Mass Spectrometry

Mass spectrometry analysis (LC/MS/MS on a Q Exactive (Thermo Scientific)) of the crosslinked products was performed at the Proteomics and Mass Spectrometry Facility of the University of Massachusetts Medical School. For quantitative analysis, raw data files were processed with Mascot Distiller (version

2.5) prior to searching with Mascot Server (version 2.4) against the *Chlamydomonas* index of NCBInr. Search parameters used were fully tryptic with two missed cleavages, parent mass tolerances of 10 ppm and fragment mass tolerances of 0.05 Da. Variable modifications of acetyl (protein N-term), pyro glutamic for N-term glutamine, oxidation of methionine, and carboxymethyl cysteine were considered. Mascot Distiller's Average method was used to generate extracted ion chromatograms of precursors to determine relative protein abundances from the three most intense peptides of each protein (Silva et al., 2006).

Results

End-to-end association of ODA-DC on outer doublets

I examined subunit-subunit interactions either within the ODA-DC or between ODA-DCs, using chemical crosslinking with 1, 6-Bismaleimidohexane (BMH: a sulfhydryl-sulfhydryl crosslinker) under various conditions.

First, we treated isolated *oda6* axonemes with BMH; the crosslinked products were then solubilized and immunoprecipitated with anti-DC1 antibody. The SDS-PAGE pattern of the immunoprecipitates showed three or four major bands above the band of DC1. Mass spectrometry revealed that the band at ~230 kDa contained peptides from only DC1 and DC2 (Fig. II-1a, arrow, Fig. II-2). Although the predicted molecular masses of DC1 and DC2 are 83 kDa and 62 kDa, they migrate in SDS-PAGE with apparent masses of ~105 kDa and 70 kDa, respectively. Therefore, this product is most likely composed of one DC1 and two DC2 molecules (the combined molecular masses would be 207 kDa with an apparent mass in SDS-PAGE of ~245 kDa). In support of this possibility, BMH reacts with Cys residues, and there are two Cys in DC1 and one Cys in DC2 (Fig. II-2). Western blotting of the proteins from a high-salt extract of the crosslinked axonemes showed that the ~230-kDa product contained both DC1 and DC2 but not α- or β-tubulin (Fig. II-1b).

Second, a mixture of DC1-2-3 and porcine brain cytoplasmic

microtubules was crosslinked with BMH. In Western analysis of the high salt extract of the specimen, a band pattern similar to the one in Fig. II-1b was observed (Fig. II-1c). The resultant ~240-kDa product reacted with anti-DC1 and anti-DC2 antibodies but not with anti-tubulin antibodies. Mass spectrometry of this product revealed that it is mostly composed of DC1 and DC2, with small amount of DC3 (~4%) and ß-tubulin (<1%) (Table 1). Furthermore, a quantitative analysis of this product showed that the amount ratio of DC1 to DC2 is 0.6 (Table 1). From these results, it is most likely that these products contained one DC1 and two DC2s.

A major band at ~180-kDa was detected only with anti-DC2 antibody (Fig. II-1c, arrowhead). Consistent with this, the product is composed mostly of DC2, with small amount of DC1 (~1%), DC3 (<1%) and ß-tubulin (<0.1%) (Table 2). These results suggest that it contains two DC2s, partial DC1 and partial DC3. ~180-kDa band was also detected with anti-DC2 antibody in crosslinked axonemes, but its amount seems fewer than in the case of cytoplasmic microtubules (Fig. II-1b, arrowhead). It may be due to the difference of crosslink efficiency; the ODA-DC binds the specific site on the outer doublet microtubule, whereas it can binds to multiple position around

the cytoplasmic microtubules (see the paragraph of Quantitative binding assay).

Intriguingly, by crosslinking DC1-2 complex with BMH, the 1:2 complex of DC1-DC2 was also detected (Fig. II-1d). This result indicates that a few amount of DC1-DC2 complex dimerizes even in solution. (The slight differences in apparent masses of the 1:2 complex of DC1-DC2 in Fig. II-1a-d might be caused by different gel sizes [see Materials and Methods].) Consistent with this, in the sedimentation distribution of DC1-2-3, there was a minor peak of ~325 kDa, suggesting that a small fraction of DC1-2-3 forms dimers in solution (Fig. II-3).

As the sedimentation analysis (Fig. I-3) showed that the ODA-DC is a heterotrimer (i.e., containing only one molecule each of DC1, DC2 and DC3), the identification of crosslinked products containing two DC2s indicates that ODA-DCs associate with each other on the doublet. Furthermore, it is also suggested that self-association of the ODA-DCs does not require the presence of axonemal components other than tubulin.

Quantitative binding assay

The apparent self-association of the ODA-DCs suggests potential cooperative binding to microtubules. To explore this possibility, I quantified ODA-DC-microtubule binding by assaying co-sedimentation of DC1-2-3 with either porcine brain cytoplasmic microtubules or three kinds of *Chlamydomonas* axonemes: axonemes from wild type (in which the binding sites for the ODA-DC are fully occupied), from *oda6* (~70% occupied; Takada and Kamiya, 1994), and from *oda1* (fully available). The amount of DC1-2-3 bound to microtubules and axonemes show a dependence on the DC1-2-3 concentration that can be approximated by the Hill equation B = Bmax*F^n /(K_d +F^n), where F is the concentration of free DC1-2-3, Bmax is the saturated amount of bound DC1-2-3, n is the Hill coefficient (a measure of cooperativity), and K_d is the apparent dissociation constant (Fig. II-4). The saturated amounts of bound DC1-2-3 were in the order of cytoplasmic microtubules > *oda1* axonemes >*oda6* axonemes > wild-type axonemes, reflecting the availability of "empty" sites for the ODA-DC. From Scatchard plots of the data, the number of ODA-DCs bound to a microtubule per 24 nm was estimated to be ~0.46 for wild type, ~0.71 for *oda6*, ~1.3 for *oda1* and ~2.0 for cytoplasmic microtubules (Table 3, Fig. II-5a-d). Considering the binding to wild-type axonemes as non-specific and subtracting this value from the data derived with axonemes, the amount of ODA-DC

bound to the *oda1* axoneme would be close to 0.9; therefore ODA-DC binding to *oda1* axonemes saturates at the native wild type level (in *Chlamydomonas*, one of the nine doublets has no ODA-DC and OAD, so the averaged number of native ODA-DC molecules on wild-type axonemes is ~0.9 per 24 nm of doublet microtubule). The results are consistent with the EM observations that the ODA-DC preferentially binds to the specific site on the doublet microtubules (Fig. I-2).

The dissociation constant between DC1-2-3 and *oda1* axonemes was calculated to be 7.8×10^{-9}, which is nearly twenty times lower than that between DC1-2-3 and cytoplasmic microtubules, 1.6×10^{-7} (Table 3, Fig. II-5a-d). Therefore, the microtubule-ODA-DC affinity may be strengthened by yet unidentified factors on the doublet. The Hill coefficients of the binding curves for the *oda1* axonemes were 2.8 and that for cytoplasmic microtubules was 1.4, indicating that the binding is positively cooperative (Fig. II-6a, b).

In vitro cooperative binding to microtubules observed by microscopy

Cooperative binding between DC1-2-3 and microtubules could be directly observed by light microscopy. In the experiment shown in Fig. II-7, rhodamine-labeled cytoplasmic microtubules were mixed with different concentrations of Alexa488-labeled DC1-2-3 and observed by fluorescence

microscopy. At each concentration of labeled DC1-2-3, two classes of microtubules appeared: microtubules in one class were fully decorated with DC1-2-3 along their lengths and those in the other class were totally devoid of decoration. The percentage of decorated microtubules was increased in a dose-dependent manner: ~34% were decorated at 0.1 mM DC1-2-3, ~63% at 0.3 mM, and ~82% at 0.6 mM (The percentages of decorated microtubules were lower than those expected from the binding curve [Fig. II-4], probably because i) fluorescence labeling of the proteins decreased the binding affinity or ii) microtubules were decorated with more than one row of ODA-DCs). Thus, the binding occurred in an all-or-none manner, which also suggests positive cooperativity in the binding between DC1-2-3 and microtubules.

ODA-DC binding to axonemes in vivo

The process by which the native ODA-DC and OAD incorporate into axonemes in vivo was observed by immunofluorescence microscopy in quadriflagellated temporary dikaryons. After gametes of opposite mating types are mated, newly formed dikaryons transiently (for ~3 hours) swim with four flagella. If a mutant lacking a flagellar component is fused with a wild-type gamete, the component missing in the mutant flagella is supplied from the shared cytoplasm and the normal function thus restored. This phenomenon is called temporary dikaryon

rescue.

I first mated a double mutant *oda1oda6* (lacking both OAD and the ODA-DC) with a transformant of *oda1oda6* expressing 3×HA-tagged DC2 in order to examine the manner of binding of DC2-HA to the *oda1oda6* axonemes that initially lacked the ODA-DC. I found that the signal of DC2-HA first appeared in the proximal part and then proceeded to the distal part of the *oda1oda6* axonemes (Fig. II-8a). The fact that assembly extends unidirectionally from proximal to distal indicates that ODA-DCs newly incorporated into the axoneme bind next to ODA-DCs that are already there, consistent with strong cooperative binding.

I next mated wild type with *oda1*. In these dikaryons, the flagella originating from the *oda1* gamete lack both the ODA-DC and OAD; both must be supplied from the wild-type cytoplasm. The progression of OAD binding to the *oda1* axoneme, as monitored by the signal of the OAD intermediate chain IC2, was similar to that of DC2-HA (Fig. II-8b) – e.g., it proceeded strictly from proximal to distal. Since 1) the ODA-DC and OAD are transported separately within flagella (Wakabayashi et al., 2001), 2) ODA-DC incorporation into the axoneme proceeds from base to tip (previous paragraph), and 3) OAD cannot assemble onto the axoneme in the absence of the ODA-DC (Takada and Kamiya, 1994), it is conceivable that OAD incorporation into the axoneme closely tracks ODA-DC

incorporation. These results confirm this prediction.

Finally, I mated wild type with *oda6*. In the flagella originating from the *oda6* gamete, ~70% of the ODA-DC-binding sites have been filled (based on Western blots of isolated *oda6* axonemes). In the dikaryon, the IC2 signal rapidly reached the tip of the *oda6* axonemes and, with time, increased in intensity evenly along the length of the axoneme (Fig. II-8c). Therefore, OAD binding on *oda6* axonemes does not proceed in a single direction; this is in strong contrast to the binding of OAD on mutant axonemes lacking the ODA-DC, which always proceeds from base to tip. Previously, Piperno et al. (Piperno et al., 1996), studying wild type×*oda2* dikaryons, observed a similar pattern of OAD recovery in the *oda2* axonemes, which also have the ODA-DC but lack OAD. These data indicate that when OAD is incorporated into axonemes that already have ODA-DCs bound to the doublets, OAD binds without any preferred position along the axoneme.

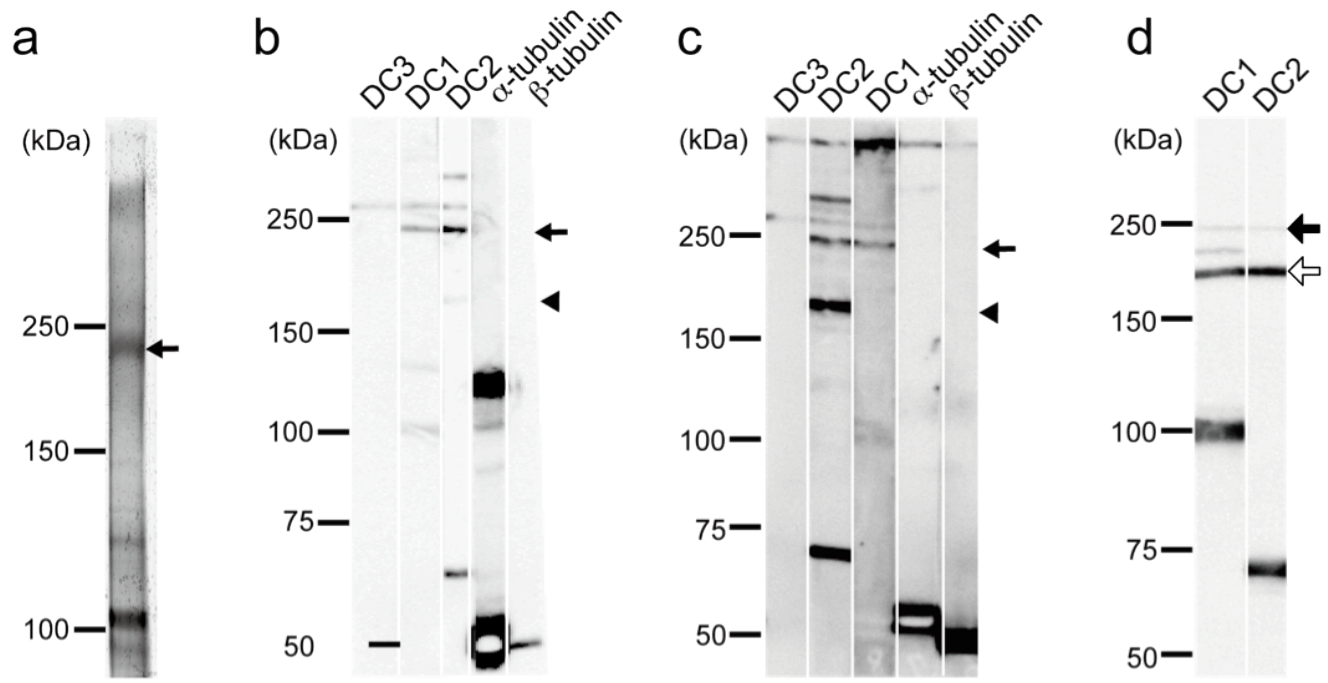

Figure II-1

(a) Silver-stained gel of anti-DC1 immunoprecipitate of products from cross-linked *oda6* axonemes. Isolated axonemes of *oda6* were crosslinked with BMH, solubilized with SDS, and the solute subjected to immunoprecipitation using the anti-DC1 antibody. Because mass spectrometry revealed that the ~230-kDa product (arrow) contained only DC1 and DC2 peptides (see Fig.II-2), the product is likely to be composed of one DC1 and two DC2s. (b-c) *oda6* axonemes (b) or cytoplasmic microtubules (c) mixed with DC1-2-3 were chemically crosslinked with BMH and the products were analyzed by Western blotting using anti-DC1, DC2, DC3, α-tubulin, and β-tubulin antibodies. An ~230-kDa product (arrow) was detected by anti-DC1 and anti-DC2 antibodies in both samples. An ~180-kDa product (arrowhead) was detected by only anti-DC2 antibody, probably because the amounts of other components were significantly smaller than that of DC2 (see Table2). (d) The DC1-2 complex in solution was chemically crosslinked with 1 μM BMH and the results analyzed in a Western blot probed with anti-DC1 and anti-DC2 antibodies. Two products (~240 kDa, filled arrow; ~190 kDa, open arrow) were detected by both antibodies. Based on the apparent molecular weights of DC1 and DC2, it seems likely that the former is composed of one DC1 and two DC2s, and the latter is composed of one DC1 and one DC2.

a

DC1

```
  1 maqkstlklp rlrtkeellk tspelckllg edsddgrsms pftapppagt vkppsrglpa
 61 vstkatkgpg mdtprglgee elteeellrl elekiknerq vlldsiklvk aqagtaggea
121 qgndikalrr elelkkakln elhedvrrke nvlnkgrddt tdasrltpge lseeqayiqq
181 lqdemkqide elveaeaknr lyyllgertr rehlamdmkv rasqqlkkds addlytltah
241 fnemraakeq aerelarmkr mleetrvdwq kklrerrrev relkkrqqkq lererkmrek
301 qlererqere lqaklkmeqd syemrvaala pkveamehsw nrirtisgad tpeevlaywe
361 glkakeeqmr slvslaeqre ssakseiaal lenrsgmyek gsaaaadvge gseeratlit
421 evernmegak gkfnklrsvc igaeqglrsl qerlmialee ihpdqlrash mkgghdakar
481 gkgaasagar rgsahahtpd rnkrgpatgs rsqspalvph spagdkpssp lhgtspehgh
541 epipegaeel ageaemvspl gadgntidde hffpelpell tsvtdrlnrv lvlaaeldaq
601 epagagedgl plsgepgadg aegaapasps rgapeglses ertlvkgmnr rtwtgaplle
661 tinaspseaa ltlnikrkkg kkkeqqvqpd lnrilgytgs dveeeepese eeteeeankd
```

DC2

```
  1 mpsadatrgg gsagsmgkgt lgagdtlghk svldkqraai eklraqneql ktelllenkf
 61 svrpgdpfaq alinrlqdeg dmlarkivle mrktkmldqq lsemgstltt trnnmggifs
121 akeqstavqk rikllenrle kayvkynqsi thnkqlresi nnlrrerimf esiqsnlere
181 laklkrdmad miqqangafe arekaigemn alkaqadkeq qgfeeewrql ttiieedkke
241 reraraqela mreretqell kmgtlssaek kkritkgswn vgynkamaqn vaaekvemyg
301 qafkriqdat giedidqlvn tflaaedqny tlfnyvnevn qeiekledqi nimrgeinky
361 retgreldmt ksrelteeea rlaaseaqsq lyekrtdsal smttalkagi ndlferiggn
421 tpavrdllge egvteanlta ylgiieqrtn eilqiyakrk aqqgtdglae allaqpltqp
481 gnriiiepps ttqeeevegl epepveedrp ltrehleskv qrtlprklet aikvrpagad
541 atggkrgspt rr
```

b

Peptide detected by MS (DC1)

K.QLERER.Q + Gln->pyro-Glu (N-term Q)
R.EHLAMDMK.V
R.QERELQAK.L + Gln->pyro-Glu (N-term Q)
R.SLVSLAEQR.E
R.LYYLLGER.T
K.SEIAALLENR.S
K.EQQVQPDLNR.I
K.VEAMEHSWNR.I
K.NRLYYLLGER.T
K.EQAERELARMK.R + Oxidation (M)
K.LKMEQDSYEMR.V
R.MLEETRVDWQK.K
R.SLVSLAEQRESSAK.S
K.AQAGTAGGEAQQNDIK.A
R.LMIALEEIHPDQLR.A
R.LMIALEEIHPDQLR.A + Oxidation (M)
R.VAALAPKVEAMEHSWNR.I + Oxidation (M)
K.DSADDLYTLTAHFNEMR.A
K.DSADDLYTLTAHFNEMR.A + Oxidation (M)
R.TISGADTPEEVLAYWEGLK.A

Peptide detected by MS/MS (DC1)

K.VEAMEHSWNR.I

Peptide detected by MS (DC2)

M.PSADATR.G + Acetyl (Protein N-term)
R.AQELAMR.E
K.AGINDLFER.I
R.ARAQELAMR.E
K.GTLGAGDTLGHK.S
K.LEDQINIMR.G
R.LQDEGDMLAR.K
R.TNEILQIYAKR.K
R.IMFESIQSNLER.E
R.IMFESIQSNLER.E + Oxidation (M)
R.LAASEAQSQLYEKR.T
R.DMADMIQQANGAFEAR.E
K.FSVRPGDPFAQALINR.L
K.AQADKEQQGFEEEWR.Q
R.ETQELLKMGTLSSAEKK.K + Oxidation (M)
K.MLDQQLSEMGSTLTTTR.N

Peptide detected by MS/MS (DC2)

R.IMFESIQSNLER.E
R.DMADMIQQANGAFEAR.E
K.AQADKEQQGFEEEWR.Q

Figure II-2

(a) The amino acid sequences of DC1 and DC2. The peptides detected by mass spectrometry of the ~230 kDa product in Figure II-1a are highlighted (yellow boxes: some peptides were overlapped). The cysteine residues are highlighted with purple boxes. (b) The all peptides detected by mass spectrometry.

Table 1

Quantitative analysis of proteins in the ~240-kDa product in Fig. II-1c

	*Score	Mass	**Amount(%)
DC2	7782	62223	100
DC1	5226	83440	60.943
DC3	815	21556	3.813
β-tubulin	147	50157	0.137

*Score values represent the summation of individual Mascot scores for identified peptides.

** Amount values represent relative ratios, with the most abundant protein normalized to 100 by Mascot Distiller (method: Average).

Table 2

Quantitative analysis of proteins in the ~180-kDa product in Fig. II-1c

	*Score	Mass	**Amount(%)
DC2	9221	62223	100
DC1	1642	83440	1.309
DC3	516	21556	0.951
β-tubulin	178	50157	0.034

*Score values represent the summation of individual Mascot scores for identified peptides.

**Amount values represent relative ratios, with the most abundant protein normalized to 100 by Mascot Distiller (method: Average).

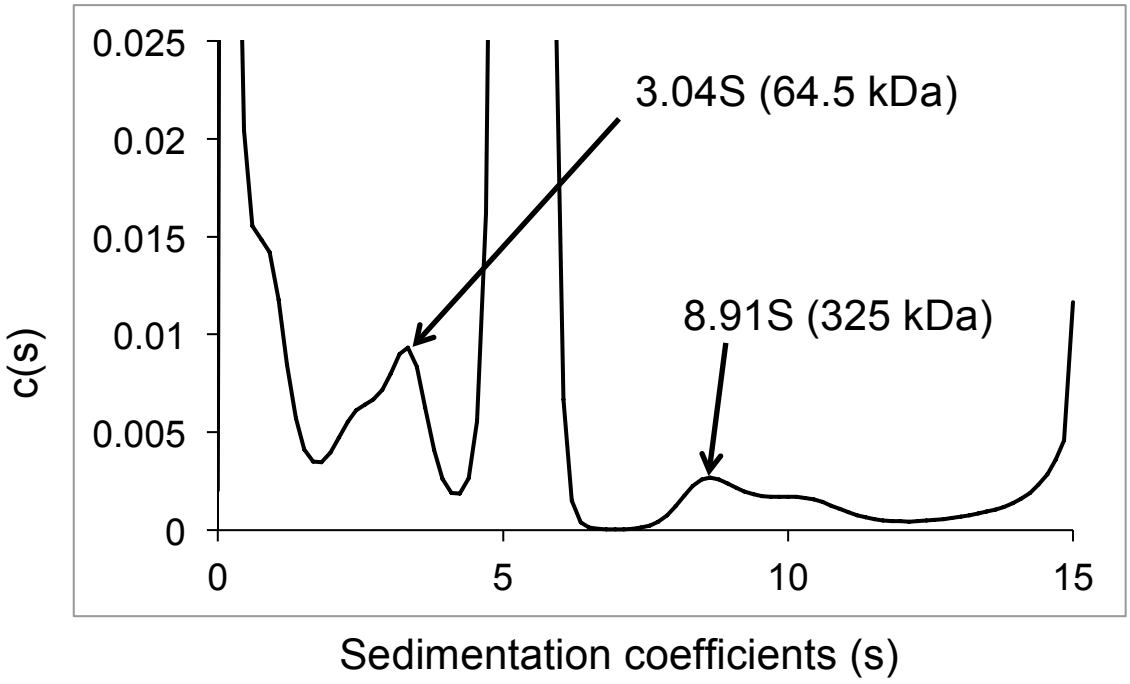

Figure II-3

There were two minor peaks in Figure I-3. 2.74% of the solutes had an S-value of 3.04S (64.5 kDa), which is close to the molecular mass of DC2 (62,204 Da). This peak most likely reflects DC2-6×His that was purified by Ni-NTA but did not form a complex with DC1 or DC3. 0.43% of the solutes had an S-value of 8.91S (325 kDa), which is close to twice the sum of the molecular masses of DC1, DC2 and DC3 (333,850 Da). This peak suggests that a small fraction of the DC1-2-3 complexes formed dimers.

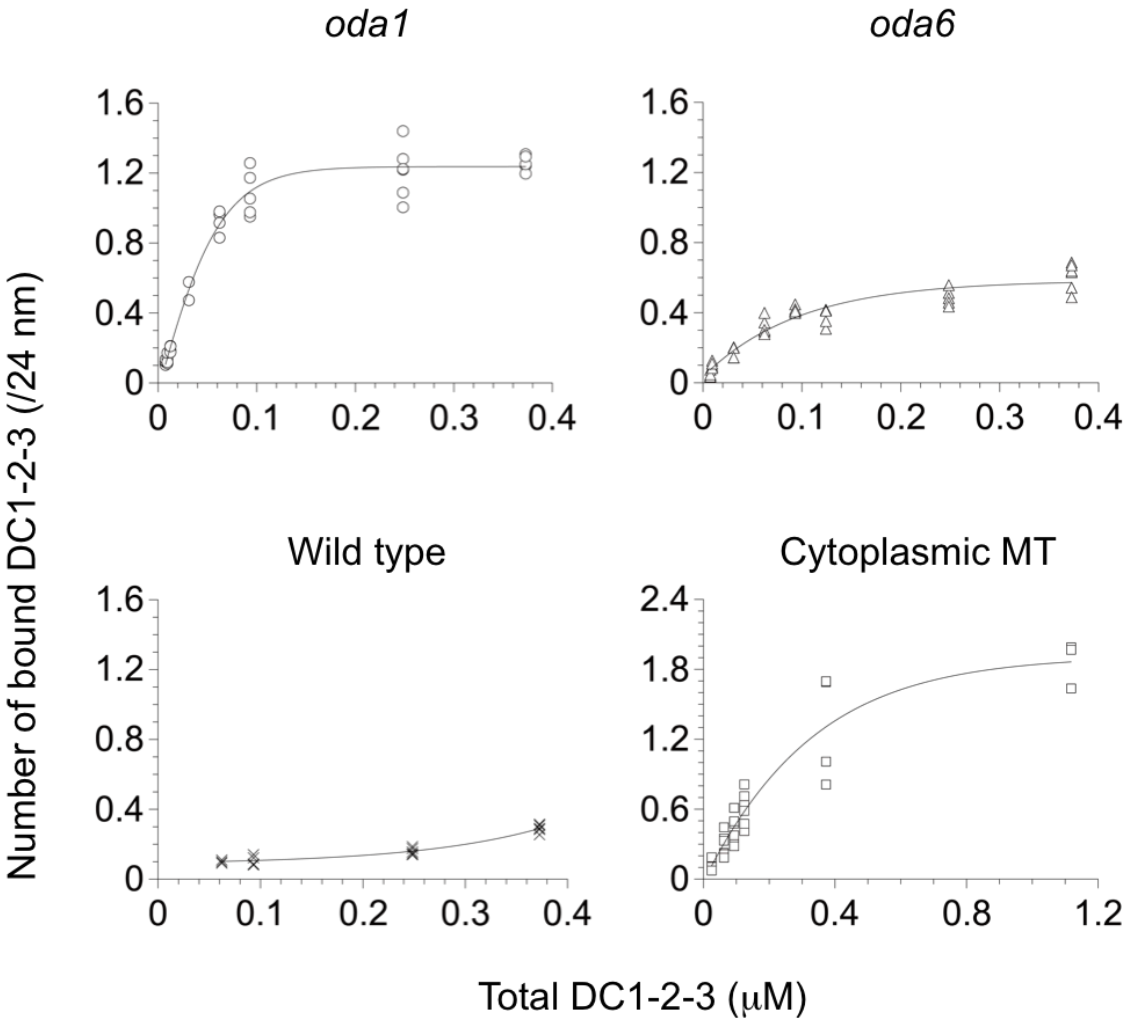

Figure II-4

Binding between DC1-2-3 and axonemes or cytoplasmic microtubules was analyzed by co-sedimentation assay. Purified DC1-2-3 was mixed with axonemes of *oda1*, *oda6*, and wild-type cells, and with porcine brain cytoplasmic microtubules. The amount of bound DC1-2-3 was calculated as the number of molecules bound to microtubules per 24 nm (Y axis), and plotted against total DC1-2-3 (X axis). The saturated amount of bound DC1-2-3 was in the order of cytoplasmic microtubules>*oda1*>*oda6*>wild type, reflecting the available sites for ODA-DC binding.

Table 3

Parameters of DC1–2–3 binding to microtubules

Microtubules used for co-sedimentation	***Kd* (M)**	**Bmax: μM / number of molecules per 24 nm**
***oda1* axonemes**	**7.8×10^{-9}**	**0.069 / 1.3**
***oda6* axonemes**	**6.1×10^{-8}**	**0.037 / 0.71**
Wild-type axonemes	**2.5×10^{-7}**	**0.024 / 0.46**
Cytoplasmic Microtubules	**1.6×10^{-7}**	**0.26 / 2.0**

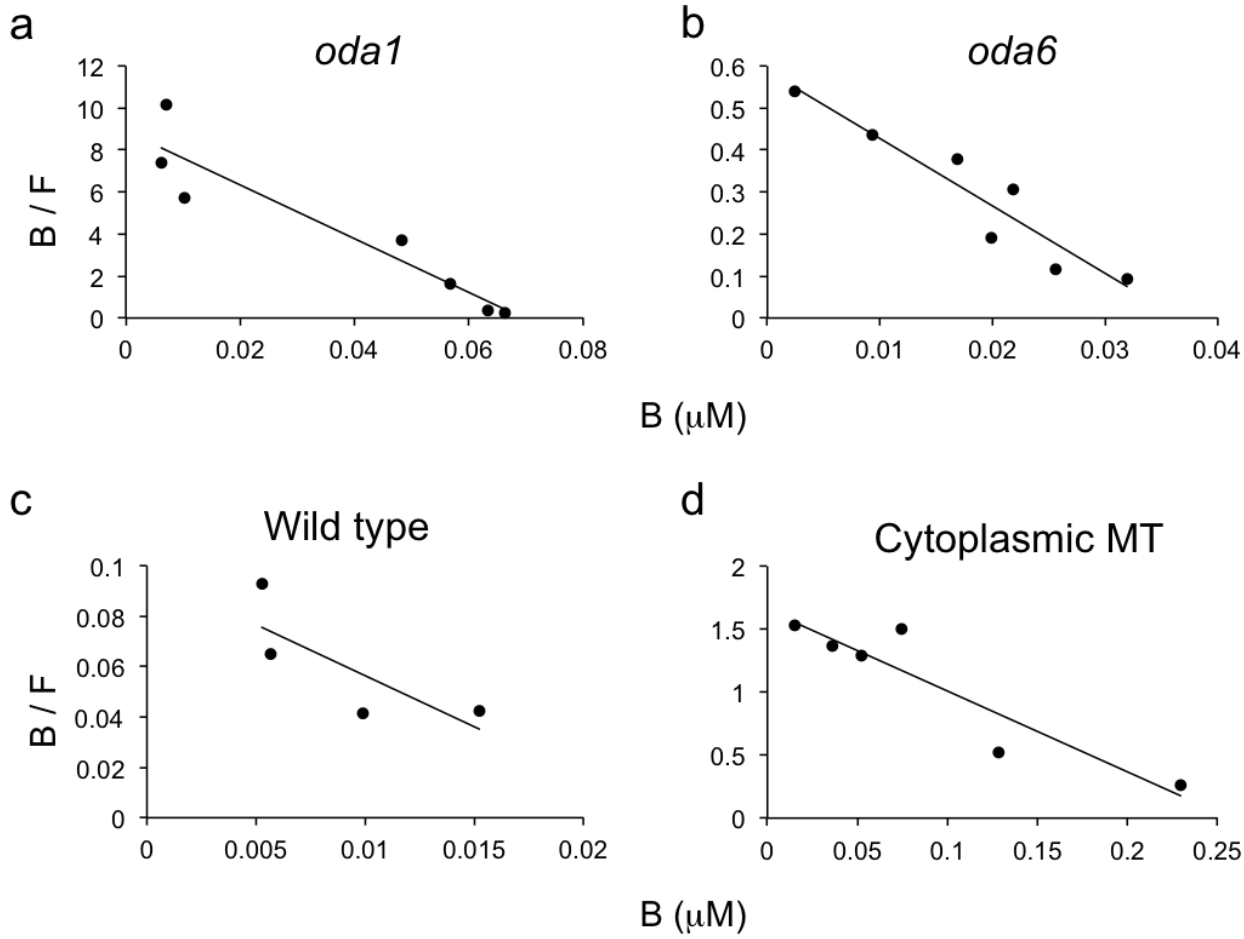

Figure II-5

Scatchard plot analyses of binding data between DC1-2-3 and (a) *oda1* axonemes, (b) *oda6* axonemes, (c) wild type axonemes, and (d) porcine brain cytoplasmic microtubules. Bound (B)/ free (F) was plotted against bound (B). Kd and Bmax are (a) 7.8×10^{-9} M and 0.069 μM, (b) 6.1×10^{-8} M and 0.037 μM, (c) 2.5×10^{-7} M and 0.024 μM, and (d) 1.6×10^{-7} M and 0.26 μM.

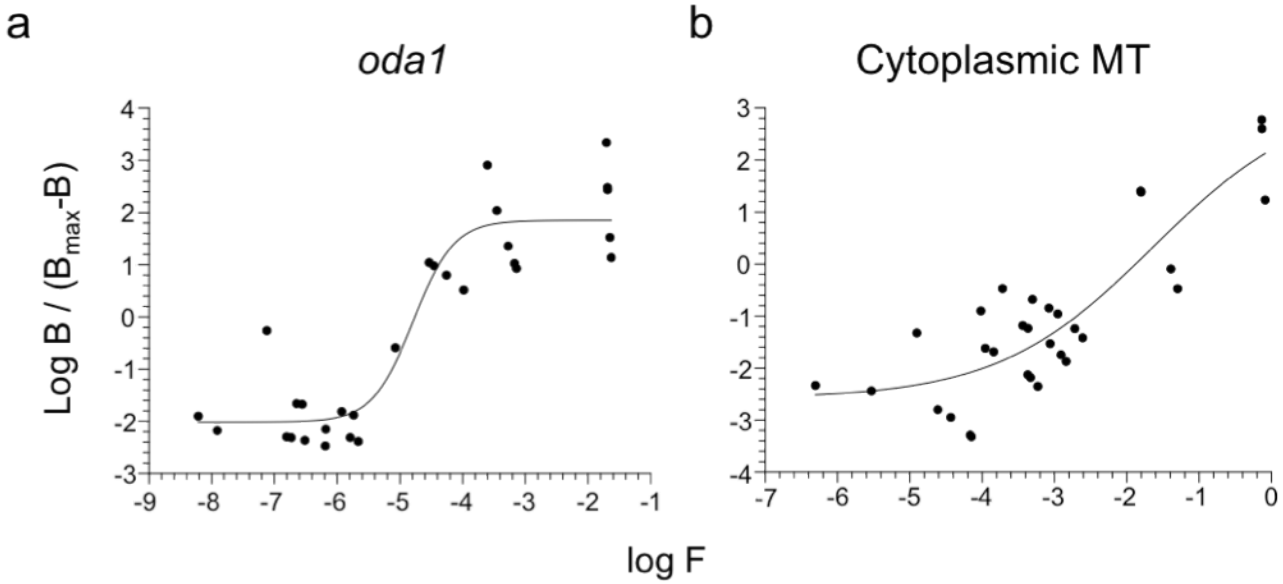

Figure II-6

Hill plot analyses of binding between (a) DC1-2-3 and oda1 axonemes, and (b) DC1-2-3 and porcine brain cytoplasmic microtubules. Log B / (Bmax-B) was plotted against log F. Hill coefficients derived from the fits are (a) 2.8 and (b) 1.4, suggesting positively cooperative interactions.

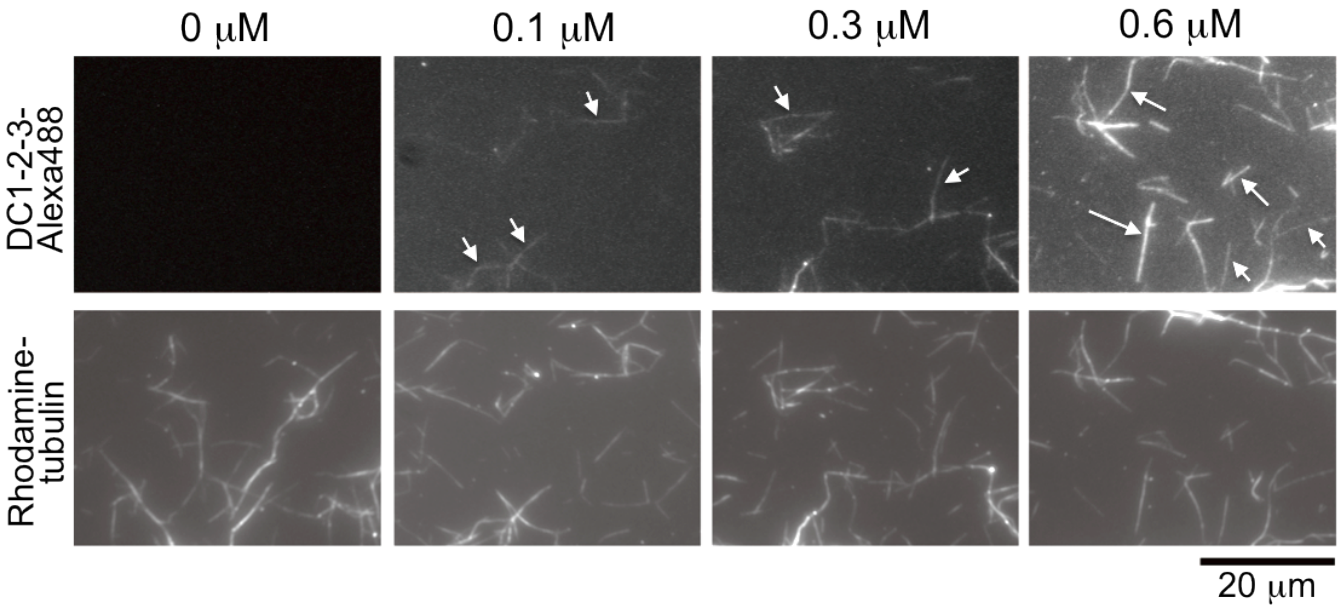

Figure II-7

Different concentrations of Alexa488-labeled DC1-2-3 were mixed with Rhodamine-labeled microtubules and observed by fluorescence microscopy. At 0.1 μM DC1-2-3, some microtubules were labeled whereas others were not at all. At 0.3 μM more microtubules were labeled but some remained unlabeled. At 0.6 μM almost all microtubules in the panel were labeled. Lengths of arrows in the upper panels represent the fluorescence intensity, and microtubules marked with the same size of arrows have similar intensities. (Shortest arrows are ~30 (arbitrary unit), mid arrows 60~70, and the longest arrow ~87.)

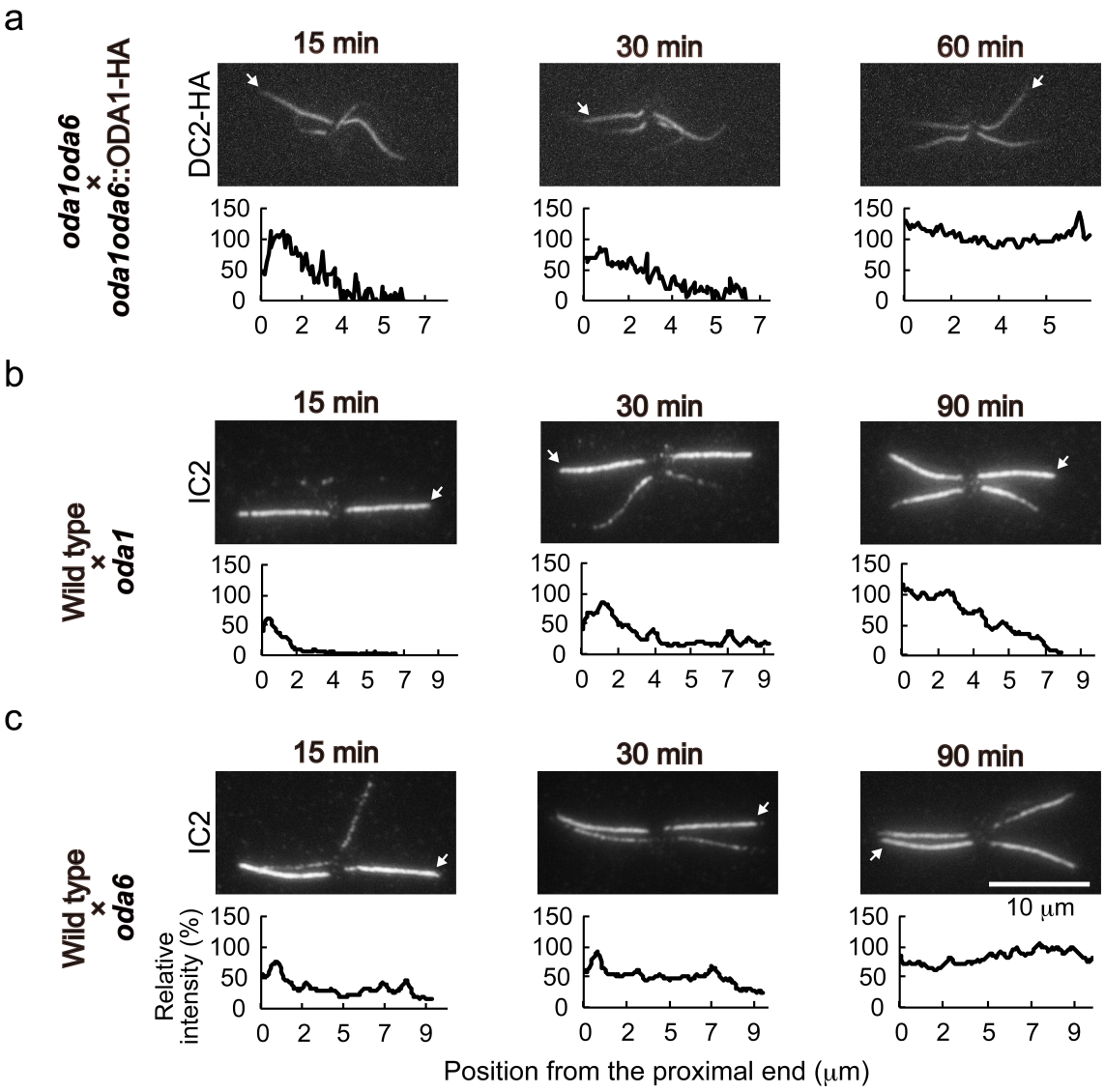

Figure II-8

(a-c upper panels) Immunofluorescence staining of temporary dikaryons: (a) *oda1oda6* × *oda1oda6*::ODA1-HA expressing DC2-3×HA, (b) wild type × *oda1*, and (c) wild type × *oda6*. The time after mating is noted on each picture. Dikaryons were demembranated and labeled with (a) anti-HA or (b, c) anti-IC2 antibody. (a-c lower panels) The fluorescence intensity of DC2-HA or IC2 in axonemes originally lacking those proteins was normalized respectively with that of *oda1oda6*::ODA1-HA (a, arrows) or wild-type (b, c, arrows) axonemes in the same dikaryon. (go to next page)

d

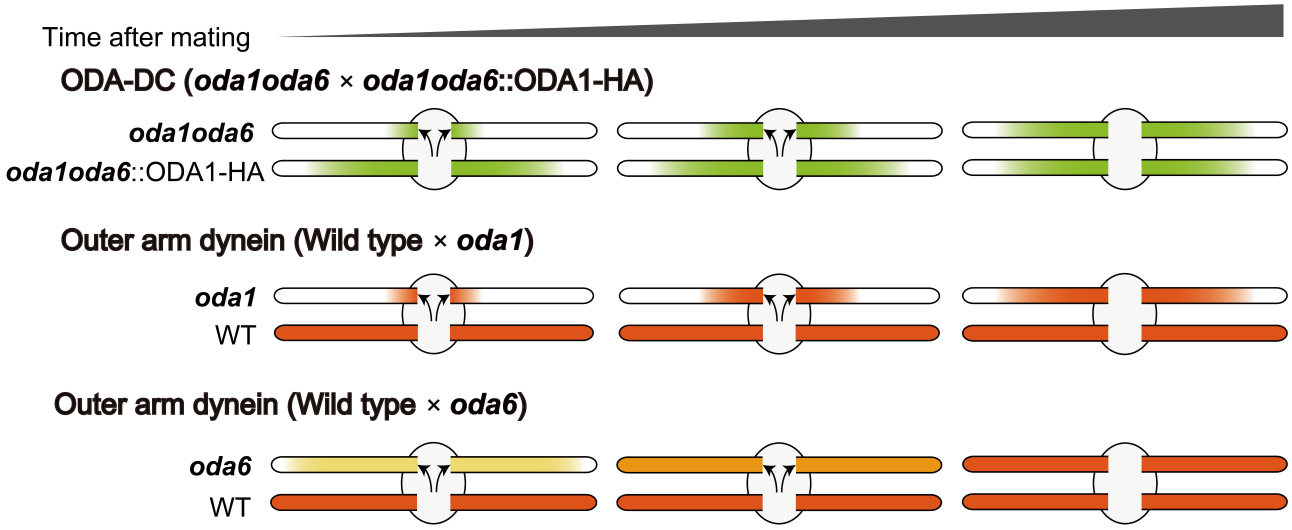

(a) Binding of the HA-tagged ODA-DC proceeded from the proximal part of the *oda1oda6* axoneme to the distal part. (b) Similarly, binding of OAD proceeded from proximal to distal in the *oda1* axoneme. (c) In contrast, binding of OAD gradually increased over the whole length of the *oda6* axoneme. The difference is that the ODA-DC was already present on the doublets of the *oda6* axonemes but not on the doublets of the *oda1* axonemes; hence, ODA assembly was constrained to follow the pattern of ODA-DC assembly in the *oda1* axonemes. (d) Schematic diagrams illustrating patterns of labeling for the ODA-DC (green) and the OAD (shades of orange) in the experiments of (a-c).

Discussion

In this part, I examined the microtubule-binding properties of the ODA-DC. I found that the ODA-DC is bound to the outer doublet in an end-to-end manner. By binding assays between DC1-2-3 and cytoplasmic/axonemal microtubules, I also found that the binding is positively cooperative (Fig. II-5), and the end-to-end binding does not require any other axonemal proteins (Fig. II-1). Furthermore, the analytical ultracentrifugation data and chemical crosslinking of DC1-2 complex revealed that the ODA-DCs associate weakly even in solution (Fig. II-3). This self-association property may produce the positively cooperative binding to the microtubule. Co-sedimentation assays indicated that the affinity and cooperativity of DC1-2-3 binding to the doublet is much higher than to the cytoplasmic microtubule (Table 3). As suggested in Part I, this result also implies that some yet unidentified factor(s) specify the site.

When Alexa-488-labeled DC1-2-3s bound to a microtubule, they apparently bound along the entire length of the microtubule (Fig. II-7). This indicates that once ODA-DCs begin to bind to a microtubule, the binding rapidly extends the entire length of the microtubule. Intriguingly, in Fig. II-7, some of the microtubules were decorated by possibly two or three tracks of DC1-2-3 in 0.6 μM, whereas such strongly labeled microtubules were not observed at the lower

concentrations. These data suggest that microtubules decorated with DC1-2-3 along their length have lower affinity for DC1-2-3 than bare microtubules. One possibility is that the binding of ODA-DC to microtubules in lateral directions is negatively cooperative: e.g., once an ODA-DC molecule is bound to a protofilament, the binding of other ODA-DCs to the adjacent protofilaments is inhibited. This phenomenon, together with the unidentified axonemal factor(s), may contribute to ensuring the arrangement of ODA-DC on the doublet in a single row.

The Bmax of bound DC1-2-3 is ~2.0 molecules per 24 nm (Fig. II-5d, Table 3). In contrast, a previous study showed that averaged ~4 outer dynein arms attached to the microtubule per transverse section of EM when high-salt extracts were added to the brain microtubules (Haimo and Fenton, 1984). Although the reason for this apparent discrepancy is not understood, one possibility is that the Bmax was underestimated due to the difficulty to measure microtubule-binding with high concentration of DC1-2-3.

Immunofluorescence observation of temporary dikaryons mated *oda1oda6* with *oda1oda6*::ODA1-HA showed that the ODA-DC starts binding to the axoneme in the proximal portion, and the binding proceeds to the distal part

(Fig. II-8a). Considering that ODA-DCs associate with each other in situ and bind to the axoneme cooperatively in vitro, this unidirectional progression is most likely mediated by the cooperative binding between the outer doublet and the ODA-DC in vivo.

In spite of the high affinity and cooperativity of binding between *oda1* axonemes and DC1-2-3 in vitro shown in Table 3, the development of the DC2-HA signal intensity (in Fig. II-8a) was slower than expected (it took ~60 min to be saturated). This is most likely because the supply of the ODA-DC into the flagellum is rate limiting. A previous study found the interaction between the ODA-DC and IFT in matrix region of flagella (Qin et al., 2004). However, we observed that the manner in which the ODA-DC is incorporated into the axoneme in vivo is quite different from that of some other structures – specifically radial spokes and inner arm dyneins – that are transported by IFT: they start binding at the flagellar tip and binding then proceeds proximally (Johnson and Rosenbaum, 1992; Piperno et al., 1996). The ODA-DC may require IFT for entry into flagella and be released from the IFT system soon after entry, whereas the radial spokes and inner dynein arms may be more tightly bound to IFT particles and be released at the tip of the flagellum. Alternatively, the ODA-DC may enter the flagellum by some IFT-independent system, since *ift46* mutant flagella, which have greatly

reduced amounts of IFT complex B (functioning in anterograde IFT), retain the ODA-DC but not OAD (Hou et al., 2007). In either case, slow incorporation of the ODA-DC should contribute to the unidirectional binding of the ODA-DC to the axoneme.

General Discussion

Most of the axonemal components are arranged periodically on the outer doublet /central pair of microtubules, but the basis of regular arrangement has been poorly understood. In this study, I focused on OAD, the most powerful axonemal dynein that binds to the outer doublet every 24 nm.

A previous study has demonstrated that when a high-salt extract from *Chlamydomonas* wild type axonemes was mixed with porcine brain microtubules, OAD orderly attached to the microtubules with a periodicity of 24 nm (Haimo et al., 1979). This arrangement was thought to be accomplished by self-interaction of OAD, which is ~24 nm in length. However, it must be noted that the high salt extract from wild-type axonemes contains both OAD and ODA-DCs. As described in this study, the ODA-DC has a property to bind to the microtubule in a cooperative manner. It is most likely that the cooperative arrangement of the ODA-DC is responsible for the regular arrangement of OAD.

From the data obtained in this and previous studies, I propose a model that explains the periodic arrangement of OAD on the outer doublet (Fig. 2). First, OAD and the ODA-DC are assembled in the cytoplasm independently of each other, and separately transported to the flagella (Fowkes and Mitchell, 1998; Wakabayashi et al., 2001). After entry into the flagella, the ODA-DC, 24 nm in

length, starts binding to appropriate sites at the proximal end of doublet microtubules. The ODA-DC molecules cooperatively bind to the doublet in an end-to-end manner and establish a 24-nm periodicity. Subsequently, OAD binds to the outer doublet through its association with the ODA-DCs on the doublet, and this interaction is stabilized through the direct interaction of IC1 with the microtubule, thereby establishing the 24-nm periodicity in the OAD arrangement (DiBella et al., 2004; Ide et al., 2013; King et al., 1995; King et al., 1991).

This study suggests that the ODA-DC not only mediates the OAD docking to the outer doublet, but also forms a scaffold of 24-nm periodicity that ensures the regular arrangement of OAD along the doublet microtubule. The length of the ODA-DC (24 nm) corresponds to that of three tubulin dimers (8×3 nm). If the ODA-DC randomly binds to any series of three tubulin dimers, a "gap" equivalent to one or two tubulin dimers would be produced between adjacent ODA-DCs. Such gaps would perturb the ordered arrangement of OAD in the 96-nm axonemal repeat and disrupt interactions between OAD and inner arm dyneins that are necessary for the coordination of force generation by the different dyneins (Nicastro et al., 2006; Oda et al., 2013). The cooperativity in the ODA-DC binding would prevent such gap formation.

To confirm the model, further structural experiments are needed such as

Cryo EM and crystallography. Those experiments will provide much information for the production of modified DC1-2-3, in order to change the 24-nm periodicity.

In this study, I revealed that the ODA-DC functions as the molecular basis of outer arm periodicity. A similar mechanism may underlie the periodic-binding of other axonemal structures, such as inner arm dyneins and radial spokes.

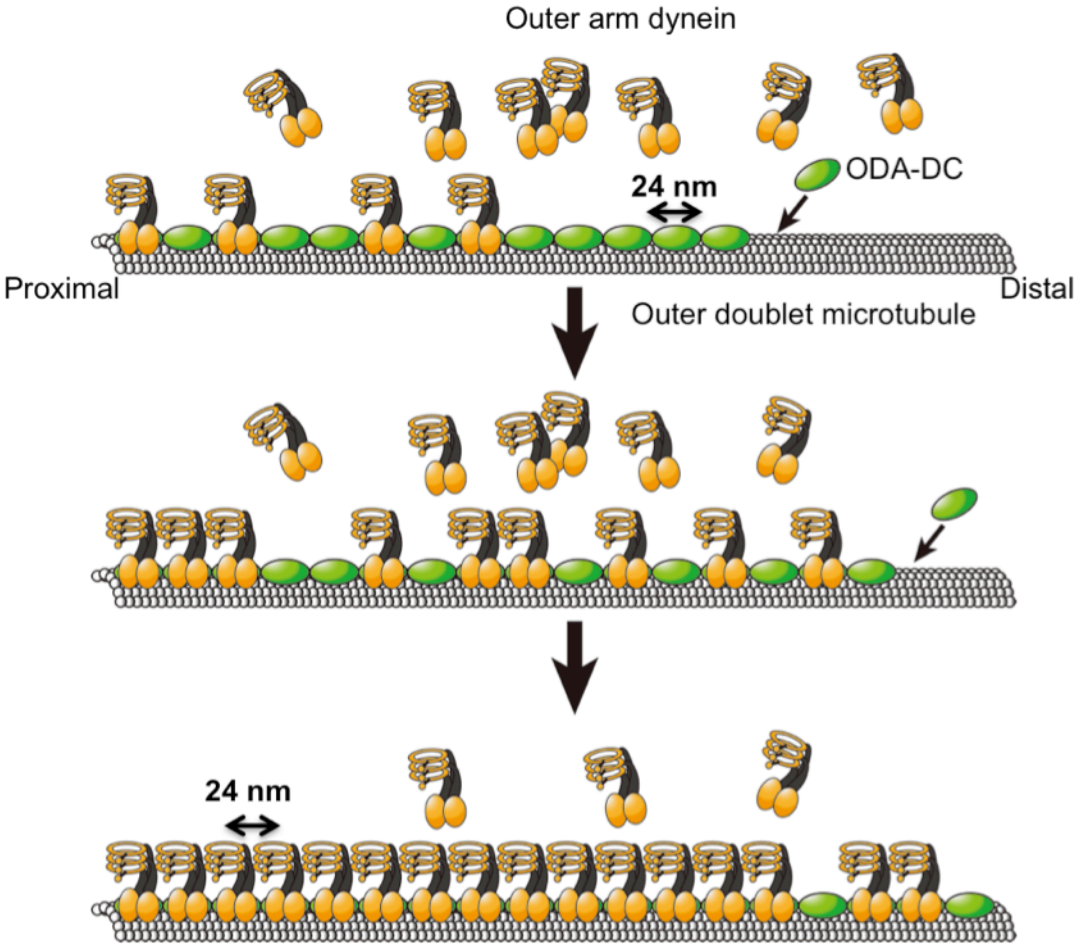

Figure 2

The ODA-DC cooperatively binds to the outer doublet from the proximal part of the axoneme to the distal part. Subsequently OAD is arranged on the “rail” of the ODA-DC. The 24-nm periodicity of OAD is based on the size of the ODA-DC.

Acknowledgements

I would like to express my sincere gratitude to my supervisor Prof. Masafumi Hirono (Univ. Tokyo) for his encouragement, giving me valuable suggestions and the opportunity to study in his laboratory. I am deeply grateful to Prof. Ritsu Kamiya for giving me the opportunity to study on cilia and flagella and his encouragement, Dr. Ken-ichi Wakabayashi (Tokyo Tech) for his guidance, encouragement, and instruction in various experimental methods and techniques. Discussion with them has always stimulated me to study energetically throughout Ph.D course.

I also thank Prof. Jiro Usukura for rotary shadowing of DC1-2-3, Prof. Fumio Arisaka for ultracentrifugation analysis of DC1-2-3, Dr. John Leszyk (UMMS) for mass spec analysis, Prof. Stephen M. King for giving helpful advice in chemical crosslinking experiments, Dr. Haru-aki Yanagisawa (Univ. Tokyo) for assistance in generating the transformant expressing HA-tagged DC2, Drs. Masahito Hayashi (Nagoya Univ.) and Takahiro Ide (Tokyo Tech) for giving helpful advice in the protein introduction by electroporation, Prof. George B. Witman (UMMS) for giving significant suggestions, and Dr. Yuqing Hou (UMMS) for helpful discussion.

References

Ahmed, N. T., C. Gao, B. F. Lucker, D. G. Cole and D. R. Mitchell. 2008. ODA16 aids axonemal outer row dynein assembly through an interaction with the intraflagellar transport machinery. *J Cell Biol*. 183:313-322.

Afzelius, B.A. 2004. Cilia-related diseases. *J Pathol*. 204:470-477.

Bloodgood, R.A. 2010. Sensory reception is an attribute of both primary cilia and motile cilia. *J Cell Sci*. 123:505-509.

Brokaw, C.J. 1994. Control of flagellar bending: a new agenda based on dynein diversity. *Cell Motil Cytoskeleton*. 28:199-204.

Brokaw, C.J. and R. Kamiya. 1987. Bending patterns of Chlamydomonas flagella: IV. Mutants with defects in inner and outer dynein arms indicate differences in dynein arm function. *Cell Motil Cytoskeleton*. 8:67-85.

Bui, K.H., H. Sakakibara, T. Movassagh, K. Oiwa, and T. Ishikawa. 2009. Asymmetry of inner dynein arms and inter-doublet links in Chlamydomonas flagella. *J Cell Biol*. 186:437-446.

Casey, D., T. Yagi, R. Kamiya, and G. Witman. 2003a. DC3, the smallest subunit of the Chlamydomonas flagellar outer dynein arm-docking complex, is a redox-sensitive calcium-binding protein. *J Biol Chem*. 278:42652-42659.

Casey, D.M., K. Inaba, G.J. Pazour, S. Takada, K. Wakabayashi, C.G. Wilkerson, R. Kamiya, and G.B. Witman. 2003b. DC3, the 21-kDa subunit of the outer dynein arm-docking complex (ODA-DC), is a novel EF-hand protein important for assembly of

both the outer arm and the ODA-DC. *Mol Biol Cell*. 14:3650-3663.

Castoldi, M., and A.V. Popov. 2003. Purification of brain tubulin through two cycles of polymerization-depolymerization in a high-molarity buffer. *Protein Expr Purif*. 32:83-88.

DiBella, L.M., M. Sakato, R.S. Patel-King, G.J. Pazour, and S.M. King. 2004. The LC7 light chains of Chlamydomonas flagellar dyneins interact with components required for both motor assembly and regulation. *Mol Biol Cell*. 15:4633-4646.

Fliegauf, M., T. Benzing, and H. Omran. 2007. When cilia go bad: cilia defects and ciliopathies. *Nat Rev Mol Cell Biol*. 8:880-893.

Fowkes, M.E., and D.R. Mitchell. 1998. The Role of Preassembled Cytoplasmic Complexes in Assembly of Flagellar Dynein Subunits. *Mol Biol Cell*. 9:2337-2347.

Goodenough, U., and J. Heuser. 1984. Structural comparison of purified dynein proteins with in situ dynein arms. *J Mol Biol*. 180:1083-1118.

Gorman, D.S., and R.P. Levine. 1965. Cytochrome f and plastocyanin: their sequence in the photosynthetic electron transport chain of Chlamydomonas reinhardi. *Proc Natl Acad Sci U S A*. 54:1665-1669.

Haimo, L.T., B.R. Telzer, and J.L. Rosenbaum. 1979. Dynein binds to and crossbridges cytoplasmic microtubules. *Proc Natl Acad Sci U S A*. 76:5759-5763.

Haimo, L.T. and R.D. Fenton. 1984. Microtubule crossbridging by chlamydomonas dynein. *Cell Motil*. 4:371-385.

Harris, E.H. 1989. The Chlamydomonas Sourcebook. Academic Press, Inc., San Diego.

Hayashi, M., HA. Yanagisawa, M. Hirono and R. Kamiya. 2002. Rescue of a Chlamydomonas inner-arm-dynein-deficient mutant by electroporation-mediated

delivery of recombinant p28 light chain. *Cell Motil Cytoskeleton*. 53:273-280.

Hou, Y., H. Qin, J.A. Follit, G.J. Pazour, J.L. Rosenbaum, and G.B. Witman. 2007. Functional analysis of an individual IFT protein: IFT46 is required for transport of outer dynein arms into flagella. *J Cell Biol*. 176:653-665.

Ide, T., M. Owa, S.M. King, R. Kamiya, and K. Wakabayashi. 2013. Protein-protein interactions between intermediate chains and the docking complex of Chlamydomonas flagellar outer arm dynein. *FEBS Lett*. 587:2143-2149.

Ishikawa, T., H. Sakakibara, and K. Oiwa. 2007. The architecture of outer dynein arms in situ. *J Mol Biol*. 368:1249-1258.

Johnson, K.A., and J.L. Rosenbaum. 1992. Polarity of flagellar assembly in Chlamydomonas. *J Cell Biol*. 119:1605-1611.

Kamiya, R. 1988. Mutations at twelve independent loci result in absence of outer dynein arms in Chlamydomonas reinhardtii. *J Cell Biol*. 107:2253-2258.

Kamiya, R. 2002. Functional diversity of axonemal dyneins as studied in Chlamydomonas mutants. *Int. Rev. Cytol*. 219:115-155.

Kamiya, R., E. Kurimoto and E. Muto. 1991. Two types of Chlamydomonas flagellar mutants missing different components of inner-arm dynein, *J. Cell Biol*. 112:441-447.

King, S.M. 2011. Composition and assembly of axonemal dyneins. *In* Dyneins: Structure, Biology and Disease. S.M. King, editor. Academic Press. 209-243.

King, S.M., R.S. Patel-King, C.G. Wilkerson, and G.B. Witman. 1995. The 78,000-M(r) intermediate chain of Chlamydomonas outer arm dynein is a microtubule-binding protein. *J Cell Biol*. 131:399-409.

King, S.M., C.G. Wilkerson, and G.B. Witman. 1991. The Mr 78,000 intermediate chain of Chlamydomonas outer arm dynein interacts with alpha-tubulin in situ. *J Biol*

Chem. 266:8401-8407.

Knowles, M.R., L.A. Daniels, S.D. Davis, M.A. Zariwala, and M.W. Leigh. 2013. Primary Ciliary Dyskinesia: Recent Advances in Diagnostics, Genetics, and Characterization of Clinical Disease. *American journal of respiratory and critical care medicine*.

Koutoulis, A., G.J. Pazour, C.G. Wilkerson, K. Inaba, H. Sheng, S. Takada, and G.B. Witman. 1997. The Chlamydomonas reinhardtii ODA3 gene encodes a protein of the outer dynein arm docking complex [published erratum appears in J Cell Biol 1997 Aug 11;138(3):729]. *J Cell Biol*. 137:1069-1080.

Laue, T.M., B.D. Shah, T.M. Ridgeway, and S.L. Pelletier. 1992. Computer-aided interpretation of analytical sedimentation data for proteins. *In* Analytical Ultracentrifugation in Biochemistry and Polymer Science. S.E. Harding, A.J. Rowe, and J.C. Horton, editors. Royal Society of Chemistry, Cambridge. 90-125.

Matsui, T., K. Hogetsu, J. Usukura, T. Sato, T. Kumasaka, Y. Akao, and N. Tanaka. 2006. Structural insight of human DEAD-box protein rck/p54 into its substrate recognition with conformational changes. *Genes to cells : devoted to molecular & cellular mechanisms*. 11:439-452.

Minoura, I., and R. Kamiya. 1995. Strikingly different propulsive forces generated by different dynein- deficient mutants in viscous media. *Cell Motil Cytoskeleton*. 31:130-139.

Mitchell, D.R., and Y. Kang. 1991. Identification of oda6 as a Chlamydomonas dynein mutant by rescue with the wild-type gene. *J Cell Biol*. 113:835-842.

Nicastro, D., C. Schwartz, J. Pierson, R. Gaudette, M.E. Porter, and J.R. McIntosh. 2006. The molecular architecture of axonemes revealed by cryoelectron tomography.

Science. 313:944-948.

Nonaka, S., Y. Tanaka, Y. Okada, S. Takeda, A. Harada, Y. Kanai, M. Kido, and N. Hirokawa. 1998. Randomization of left-right asymmetry due to loss of nodal cilia generating leftward flow of extraembryonic fluid in mice lacking KIF3B motor protein. *Cell.* 95:829 -837

Oda, T., T. Yagi, H. Yanagisawa, and M. Kikkawa. 2013. Identification of the outer-inner dynein linker as a hub controller for axonemal Dynein activities. *Curr Biol*. 23:656-664.

Omran, H., D. Kobayashi, H. Olbrich, T. Tsukahara, N.T. Loges, H. Hagiwara, Q. Zhang, G. Leblond, E. O'Toole, C. Hara, H. Mizuno, H. Kawano, M. Fliegauf, T. Yagi, S. Koshida, A. Miyawaki, H. Zentgraf, H. Seithe, R. Reinhardt, Y. Watanabe, R. Kamiya, D.R. Mitchell, and H. Takeda. 2008. Ktu/PF13 is required for cytoplasmic pre-assembly of axonemal dyneins. *Nature*. 456:611-616.

Onoufriadis, A., T. Paff, D. Antony, A. Shoemark, D. Micha, B. Kuyt, M. Schmidts, S. Petridi, J.E. Dankert-Roelse, E.G. Haarman, J.M. Daniels, R.D. Emes, R. Wilson, C. Hogg, P.J. Scambler, E.M. Chung, Uk10K, G. Pals, and H.M. Mitchison. 2013. Splice-site mutations in the axonemal outer dynein arm docking complex gene CCDC114 cause primary ciliary dyskinesia. *American journal of human genetics*. 92:88-98.

Pazour, G.J., N. Agrin, B.L. Walker, and G.B. Witman. 2006. Identification of predicted human outer dynein arm genes: candidates for primary ciliary dyskinesia genes. *J Med Genet*. 43:62-73.

Piperno, G., K. Mead, and S. Henderson. 1996. Inner dynein arms but not outer dynein arms require the activity of kinesin homologue protein KHP1(FLA10) to reach

the distal part of flagella in Chlamydomonas. *J Cell Biol*. 133:371-379.

Qin, H., D.R. Diener, S. Geimer, D.G. Cole, and J.L. Rosenbaum. 2004. Intraflagellar transport (IFT) cargo: IFT transports flagellar precursors to the tip and turnover products to the cell body. *J Cell Biol*. 164:255-266.

Sanders, M.A., and J.L. Salisbury. 1995. Immunofluorescence microscopy of cilia and flagella. *Methods Cell Biol*. 47:163-169.

Schuck, P. 2000. Size-distribution analysis of macromolecules by sedimentation velocity ultracentrifugation and lamm equation modeling. *Biophys J*. 78:1606-1619.

Silva JC, Gorenstein MV, Li GZ, Vissers JP, & Geromanos SJ (2006) Absolute quantification of proteins by LCMSE: a virtue of parallel MS acquisition. Molecular & cellular proteomics : MCP 5(1):144-156.

Sizova, I., M. Fuhrmann, and P. Hegemann. 2001. A Streptomyces rimosus aphVIII gene coding for a new type phosphotransferase provides stable antibiotic resistance to Chlamydomonas reinhardtii. *Gene*. 277:221-229.

Takada, S., and R. Kamiya. 1994. Functional reconstitution of Chlamydomonas outer dynein arms from alpha- beta and gamma subunits: requirement of a third factor. *J Cell Biol*. 126:737-745.

Takada, S., and R. Kamiya. 1997. Beat frequency difference between the two flagella of Chlamydomonas depends on the attachment site of outer dynein arms on the outer-doublet microtubules. *Cell Motil Cytoskeleton*. 36:68-75.

Takada, S., C.G. Wilkerson, K. Wakabayashi, R. Kamiya, and G.B. Witman. 2002. The outer Dynein arm-docking complex: composition and characterization of a subunit (oda1) necessary for outer arm assembly. *Mol Biol Cell*. 13:1015-1029.

Wakabayashi, K., S. Takada, G.B. Witman, and R. Kamiya. 2001. Transport and

arrangement of the outer-dynein-arm docking complex in the flagella of Chlamydomonas mutants that lack outer dynein arms. *Cell Motil Cytoskeleton*. 48:277-286.

Yagi, T., I. Minoura, A. Fujiwara, R. Saito, T. Yasunaga, M. Hirono and R. Kamiya. 2005. An axonemal dynein particularly important for flagellar movement at high viscosity. Implications from a new Chlamydomonas mutant deficient in the dynein heavy chain gene DHC9. *J Biol Chem*. 280:41412-41420.

Yoshiba, S., H. Shiratori, H., I.Y. Kuo, A. Kawasumi, K. Shinohara, S. Nonaka, Y. Asai, G. Sasaki, J.A. Belo, H. Sasaki, J. Nakai, B. Dworniczak, B.E. Ehrlich, P. Pennekamp, H. Hamada. 2012. Cilia at the node of mouse embryos sense fluid flow for left‑right determination via Pkd2 *Science*. 338:226‑231

Zariwala, M.A., M.R. Knowles, and H. Omran. 2007. Genetic defects in ciliary structure and function. *Annu Rev Physiol*. 69:423-450.